

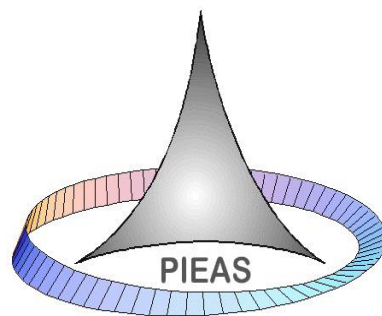
# **Abnormal Cardiac Beat Detection**

By

HASAN ASHRAF

MUNIM REHMAN KAYANI

MUHAMMAD UMER QURESHI



DEPARTMENT OF ELECTRICAL ENGINEERING,  
PAKISTAN INSTITUTE OF ENGINEERING AND APPLIED SCIENCES,  
NILORE, ISLAMABAD 45650, PAKISTAN

JUNE 2015



# Department of Electrical Engineering

Pakistan Institute of Engineering and Applied Sciences (PIEAS)

Nilore, Islamabad 45650, Pakistan

## Declaration of Originality

I hereby declare that the work contained in this thesis and the intellectual content of this thesis are the product of my own research. This thesis has not been previously published in any form nor does it contain any verbatim of the published resources which could be treated as infringement of the international copyright law. I also declare that I do understand the terms copyright and plagiarism, and that in case of any copyright violation or plagiarism found in this work, I will be held fully responsible of the consequences of any such violation.

Name

Signature

Hasan Ashraf

\_\_\_\_\_

Munim Rehman Kayani

\_\_\_\_\_

Muhammad Umer Qureshi

\_\_\_\_\_

Date: \_\_\_\_\_

Place: \_\_\_\_\_

# Certificate of Approval

*This is to certify that the work contained in this thesis entitled  
“Abnormal Cardiac Beat Detection”  
was carried out by*

**Hasan Ashraf**

**Munim Rehman Kayani**

**Muhammad Umer Qureshi**

*under my supervision and that in my opinion, it is fully adequate,  
in scope and quality, for the degree of BS Electrical Engineering from  
Pakistan Institute of Engineering and Applied Sciences (PIEAS).*

*Approved By:*

Signature: \_\_\_\_\_

Supervisor: Dr. Fayyaz ul Amir Afsar Minhas

*Verified By:*

Signature: \_\_\_\_\_

Head, Department of Electrical Engineering

Stamp:

To our parents, siblings, teachers, and colleagues

We thank you all.

## Acknowledgements

Praise be to Almighty Allah who bestowed upon us the mental faculties to contemplate the universe and gave us the strength and courage to aim for and achieve our goals.

We are very grateful to our project supervisor Dr. Fayyaz ul Amir Afsar Minhas and our co supervisor Mr. Muhammad Shahid Nazir for their guidance and help. We are grateful to Mr. Muhammad Shahid Nazir for arranging lab facilities to work on this project. We must also thank Dr. Waqas Ahmed and Dr. Muhammad Tufail, our examiners, for their time and interest.

We would like to thank Mr. Jamal Afzal and Mr. Shahzad Nadeem for providing us with laboratory facilities. Special thanks go to our colleagues Ehab ul Haq (BSEE), Ahmad Ali (BSEE), and Shafiq Ahmed (MSSE) for their technical assistance which has proved vital in the completion of this project.

# Table of Contents

Declaration of Originality .....	iii
Certificate of Approval .....	iv
Acknowledgements.....	vi
Table of Contents.....	vii
Table of Figures .....	x
Table of Tables .....	xii
Abstract.....	1
1 Introduction.....	2
1.1 Objectives and Motivation of the project.....	2
1.2 System Architecture .....	2
1.2.1 Hardware Implementation .....	3
1.2.2 Software Implementation.....	3
1.3 Organization of the Report.....	4
2 The Human Heart.....	6
2.1 Electrical Conduction System of Heart.....	6
2.1.1 Action Potentials in the Heart .....	6
2.1.2 Initiation and Propagation Action Potentials in the Heart .....	7
2.2 Measurement of Electrical Activity in the Heart .....	8
2.3 ECG Systems.....	8
2.3.1 The 12-Lead ECG System .....	8
2.3.2 Three Electrode ECG System: .....	11
2.4 ECG Waveform.....	11
2.4.1 P Wave .....	11
2.4.2 QRS Complex .....	12
2.4.3 T Wave.....	12
2.4.4 U Wave .....	12

2.4.5	PR Interval .....	12
2.4.6	QT Interval.....	13
2.4.7	ST Segment.....	13
3	ECG Acquisition.....	14
3.1	Basic Concept.....	14
3.1.1	Electrodes.....	14
3.1.2	Electrode Types .....	15
3.1.3	Amplifier.....	15
3.1.4	Filtering.....	17
3.2	ECG Acquisition System .....	18
3.2.1	Instrumentation Amplifier .....	18
3.2.2	Right Leg Drive .....	19
3.2.3	Filtering.....	19
4	Interfacing .....	20
4.1	Interfacing using USB .....	20
4.1.1	Analog to Digital Converter (ADC) .....	20
4.1.2	Universal Serial Bus (USB).....	21
4.1.3	USB Compatible Device.....	23
4.2	Interfacing using the Sound Card Input .....	27
4.1.4	Frequency Modulation .....	28
4.1.5	Voltage to Frequency Converter .....	28
4.1.6	V to F converter design.....	28
4.1.7	Interfacing with the sound card.....	31
4.1.8	Demodulation.....	32
4.2	Acquisition and interfacing circuitry.....	33
5	Artifact Removal and QRS Complex Detection.....	34
5.1	Artifact Removal .....	34



5.1.1	ECG Artifacts.....	34
5.1.2	Artifact Removal Techniques .....	34
5.1.3	Implementation and Results.....	36
5.2	QRS detection .....	37
5.2.1	The Length Transform for QRS detection.....	37
5.2.2	Implementation and Results.....	38
5.3	R wave.....	43
5.3.1	R peak detection.....	43
5.3.2	RR interval .....	43
6	Support Vector Machine for Abnormal Beat Detection .....	45
6.1	Support Vector Machines.....	45
6.2	One-class SVM .....	48
6.3	Implementation.....	48
6.3.1	Feature Extraction .....	49
6.3.2	Training and Testing .....	49
6.3.3	Evaluation .....	49
7	Conclusions and Future Work .....	51
	Appendix A.....	53
	Appendix B .....	56
	Appendix C.....	58
	Appendix D.....	60
	Appendix E .....	65
	References.....	74

## Table of Figures

Figure 1-1 Block diagram of hardware implementation.....	3
Figure 1-2 Block diagram of software implementation.....	4
Figure 2-1 Heart's Conduction System [3].....	6
Figure 2-2 Action Potentials in heart [4] .....	7
Figure 2-3 Limb lead placement [3] .....	10
Figure 2-4 Precordial lead placement [3].....	10
Figure 2-5 ECG waveform [3].....	11
Figure 3-1 Block Diagram of ECG Acquisition Circuit .....	14
Figure 3-2 Polarizable Electrode .....	15
Figure 3-3 Non Polarizable Electrode.....	15
Figure 3-4 Three Operational Amplifier Differential Amplifier Topology [6] .....	16
Figure 3-5 Block Diagram of three Lead ECG system.....	18
Figure 3-6 AD620 Circuit [5] .....	19
Figure 3-7 Leg Drive .....	19
Figure 3-8 High pass and Low pass Filters.....	19
Figure 4-1 Block Diagram for USB interface.....	20
Figure 4-2 Flow chart.....	23
Figure 4-3 Flow diagram for Main Method.....	24
Figure 4-4 Flow Diagram for the Save_File Method.....	25
Figure 4-5 Flow Diagram for the Acquire_Data Method .....	25
Figure 4-6 Flow Diagram for the Stream Method .....	26
Figure 4-7 Flow Diagram for the Real_Time_Plot Method .....	26
Figure 4-8 Sound card frequency response.....	27
Figure 4-9 Block Diagram representation of proposed system .....	28
Figure 4-10 V to F converter circuit [13].....	29
Figure 4-11 Resistive divider.....	31
Figure 4-12 Complete circuit.....	33
Figure 5-1 ECG with baseline wander and power line interference.....	35
Figure 5-2 Chebyshev bandpass filter frequency response.....	36
Figure 5-3 Raw and forward backward bandpass filtered ECG .....	37
Figure 5-4 Length transform algorithm for QRS detection .....	37
Figure 5-5 Illustration of the approximation for length transform .....	38

Figure 5-6 The preprocessed ECG filtered by a 10-25 Hz band pass filter.....	39
Figure 5-7 First order difference of the band pass filtered signal.....	39
Figure 5-8 Difference squared .....	40
Figure 5-9 Threshold values .....	40
Figure 5-10 Thresholding and potential QRS complex region.....	41
Figure 5-11 Results of morphological opening and closing .....	42
Figure 5-12 QRS fiducial points .....	42
Figure 5-13 R peak approximation .....	43
Figure 5-14 Mean RR interval plot.....	44
Figure 6-1 Data set with two types of points: hollow and filled.....	45
Figure 6-2 Support Vectors.....	46
Figure 6-3 Feature extraction.....	48
Figure 6-4 Training and testing errors .....	49
Figure A-1 ADCON0 Register .....	53
Figure A-2 ADCON1 register.....	54
Figure A-3 ADCON2 register.....	54

## Table of Tables

Table 4-1 Design Specifications .....	29
Table 4-2 DC testing of VFC circuit.....	30
Table B-1 USB wires specification.....	56

## Abstract

Cardiac diseases are the leading cause of death worldwide. Therefore there exists a need for a system that can assist the cardiologist with electrocardiogram (ECG) analysis. The project undertaken can be broken down into two separate segments. The first part is concerned with the acquisition of ECG. The second part focuses on analyzing the ECG to detect abnormalities in cardiac rhythms. The implementation of the first part incorporates an ECG acquisition circuit. The acquisition circuit includes an instrumentation amplifier, a filtering section, and an analog to digital converter and can be interfaced using a universal serial bus (USB) to any computing device. The major difficulty in ECG acquisition was line interference which required time and effort to identify and minimize. The interface to a computing device must include an Analog to Digital converter. The onboard ADC of a peripheral interface controller (PIC) was used for analog to digital conversion while the USB interface of the PIC provided an integrated solution to the interfacing problem.

An application program was written for ECG acquisition and analysis. This application communicates with the acquisition hardware through the USB interface and can be run on a PC or other device capable of USB communication. The acquired ECG is polluted by a number of artifacts the removal of which was carried out through forward backward IIR band pass filtering. The length transform algorithm was implemented for detection of QRS fiducial points and R wave peak detection. The system provides two main diagnostic utilities. First it generates a running average plot of the RR intervals which shows heart rate variability. Secondly, it implements a one-class support vector machine (SVM) for abnormal beat detection. We assume that most of the beats in the record are normal and use randomly selected beats to train the SVM. This approach has been shown to provide to Sensitivity (Se)/Specificity (Sp) of 87.6%/95.8%.

# 1 Introduction

Electrocardiogram (ECG or EKG) is a tool to measure electrical activity of the heart and we can determine the cardiac condition from the electrical activity. An in-depth analysis of ECG can indicate the type of disorder present in the heart. ECG analysis is used for timely detection of dangerous heart diseases. ECG acquisition takes place in a clinical setting and its examination is carried out by specially trained cardiac experts. Manual extraction of abnormal beats in an ECG is a painstaking process, especially in recordings of long durations. Automatic analysis of ECG is therefore of some import in biomedical signal processing.

## 1.1 Objectives and Motivation of the project

The overall objective of this project is to develop a system which acquires and analyzes an ECG signal. This system will detect basic abnormalities in cardiac rhythm like Tachycardia and Bradycardia. This acquisition system includes an interface for computing devices so as to be able to store and analyze the ECG signal.

The motivation behind development of such a system is to help medical experts in interpreting the ECG by providing a fast and reliable method of extraction of abnormalities, thus saving precious time and effort of cardiac experts. These features will help medical experts in monitoring large number of cardiac patients. This system can also be used as a teaching aid for medical and paramedical trainees. The system also incorporates features for remote acquisition and transmission of ECG over the internet and can thus be used to monitor cardiac patients at remote locations.

The importance of this system can be understood by keeping in mind that cardiovascular diseases are the leading cause of death globally [1]. In Pakistan, cardiac diseases are responsible for about 34% of annual deaths [2]. The situation is dire.

## 1.2 System Architecture

The architecture of the proposed system has the following major parts:

- 1) Hardware Implementation
- 2) Software Implementation

### **1.2.1 Hardware Implementation**

The hardware implementation can be broken down as in Figure 1-1. A brief discussion follows.

- **ECG Acquisition**

This concerns the acquisition of ECG signal from the body, keeping in mind the various sources of noise (EMI, muscle movements etc.).

- **Filtering**

Filtering is done so as to remove unwanted noise and to increase signal to noise ratio.

- **Interfacing**

This provides an interface to a computation device to store and analyze the ECG.

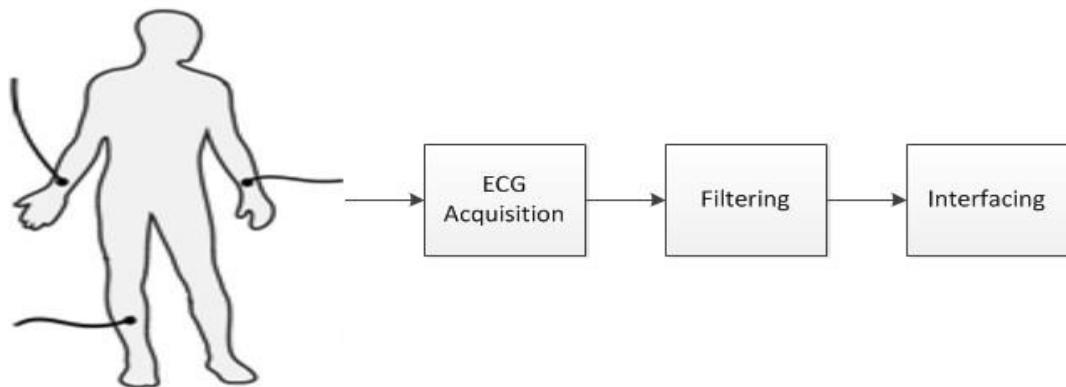


**Figure 1-1 Block diagram of hardware implementation**

### **1.2.2 Software Implementation**

Software implementation includes signal conditioning and analysis of ECG signal to extract QRS start and end points and RR intervals. It also includes a machine learning algorithm (one-class SVM) for abnormal beat detection. Figure 1-2 presents a block diagram view of the software implementation.

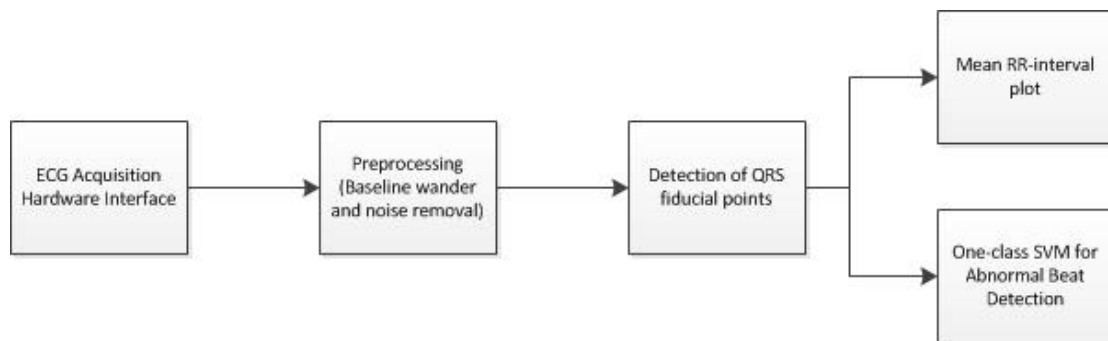


**Figure 1-2 Block diagram of software implementation**

- **Preprocessing**

To remove baseline fluctuations and power line interference from the ECG.

- **QRS detection and delineation**

This concerns the detection of QRS fiducial points and R wave peak detection.

- **Mean RR-interval plot**

One of the two diagnostic utilities provided by the software system.

- **One-class Support Vector Machine (SVM)**

This includes feature extraction and training of SVM for abnormal beat detection.

- **Logging**

This part includes data storage and report generation.

### **1.3 Organization of the Report**

This report provides a detailed description of the project and the steps involved in acquisition and interfacing of ECG signal with a computing device. Chapter 1 presents a description of the project. Chapter 2 provides basic material on the anatomy and electrical network of the heart. Chapter 3 discusses the ECG acquisition system: design and implementation. Chapter 4 describes the different methods used to



interface ECG acquisition hardware with a computation device. Chapter 5 discusses preprocessing of the ECG for noise removal and an algorithm for QRS complex detection. It also includes a discussion of R wave peak detection and the generation of mean RR interval plot. Chapter 6 delineates a method for using one-class SVM for abnormal beat detection using training data from one class. Chapter 7 presents the conclusions and discusses future work which could build upon the work contained in this thesis.

## 2 The Human Heart

This chapter describes the structure and functional working of the heart. A brief overview of the electrical activity in the heart is presented. It also provides a brief introduction to the electrocardiogram. Cardiac abnormalities are usually reflected in the ECG and an understanding of the electrical network of the heart can therefore be beneficial.

### 2.1 Electrical Conduction System of Heart

Cardiac cells contract systematically and rhythmically. The contraction of heart is a direct consequence of the contraction of all of the tiny cells of heart. These contractions of the heart cells are triggered by electric impulses generated by the Sinoatrial (SA) node within the heart as shown in Figure 2-1. The cells in the SA node depolarize resulting in a pulse which travels throughout the heart and serves as a stimulus for other cells of the heart. To understand the origin of these electrical impulses, we should be familiar with the concept of action potentials in the heart.

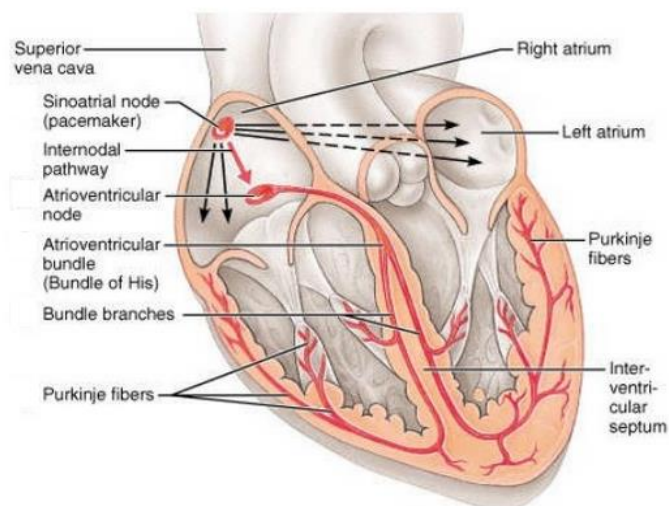


Figure 2-1 Heart's Conduction System [3]

#### 2.1.1 Action Potentials in the Heart

We know that each cell is surrounded by a semi permeable membrane known as cell membrane. The cell membrane allows ions to move in and out of the cell. Since ions are charged particles, their movement establishes a potential gradient across the cell membrane known as membrane potential. Due to this membrane potential every cell

in our body is slightly negative (at rest) inside than outside. The resting membrane potential of a cell is approximately  $-0.1$  Volt [3].

Action potential is the tendency of cells to rapidly reverse their resting membrane potential from negative value to slightly positive value which is usually known as *depolarization*. The change in potential from this slightly positive value to resting membrane potential is called *repolarization*. The cells which are capable of reversing their resting membrane potentials are called excitable cells. Cardiac cells are excitable cells. Action potentials occurring in the cardiac cells play a critical role in systematic and rhythmic beating of the heart.

### 2.1.2 Initiation and Propagation Action Potentials in the Heart

The rhythm of the heart is initiated by the action potentials generated automatically by the cells of sinoatrial (SA) node of the heart. The action potentials arising in the cells of sinoatrial (SA) node propagate to and through atrioventricular (AV) node to Bundle of His and Purkinje fibers. This propagation of action potentials through the heart synchronizes the heart. As a result, all the cells contract at the same time which results

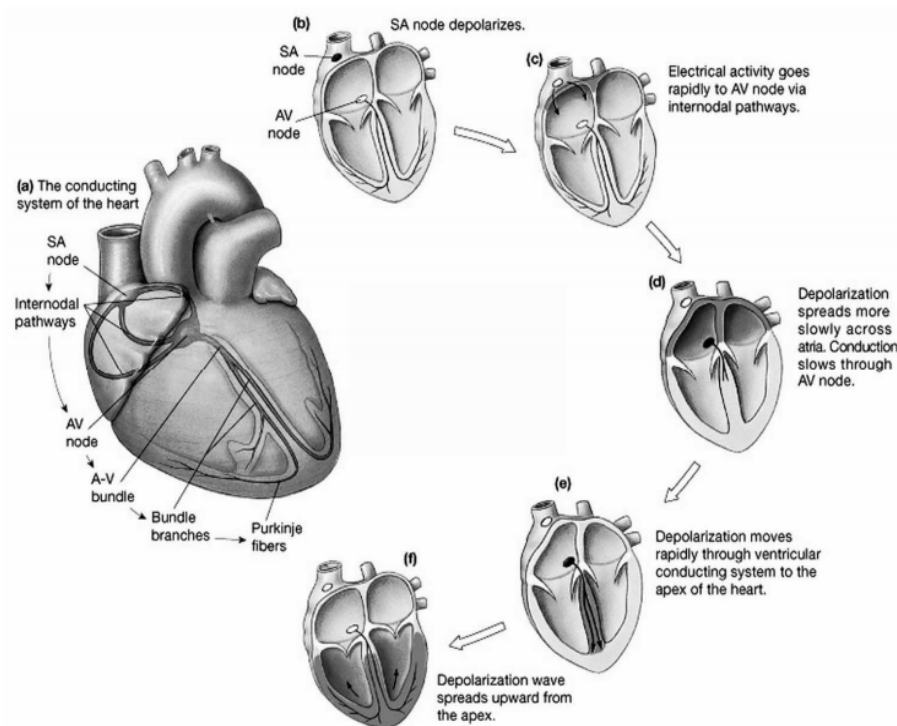


Figure 2-2 Action Potentials in heart [4]

in systematic and rhythmic beating of the heart. The initiation and transmission of action potentials in the heart is shown in Figure 2-2.

## **2.2 Measurement of Electrical Activity in the Heart**

The propagation of action potentials in the heart results in an electric pulse traveling through the heart. The characteristics of this electric pulse can be measured by using an electrocardiogram (ECG). The electrocardiogram is an indirect way of measuring the electrical activity in the heart. A device for recording ECG was invented by William Einthoven in 1901.

An electrocardiogram is obtained by measuring the potential difference between different points on the body. A detailed analysis of the heart's electrical activity can be carried out by studying the ECG which also helps in the diagnosis of various cardiac disorders.

## **2.3 ECG Systems**

Electrodes placed on the skin, which are used to obtain an electrocardiogram, provide a view of the heart's electrical activity in the shape of a waveform. An ECG records these waveforms from different perspectives called planes and leads.

A *lead* provides a view of the heart's electrical activity between a positive and a negative pole. The two poles define the lead's axis. The term "axis" refers to the direction of the current moving through the heart. The direction of the current affects the direction of the ECG waveform. If the current is moving towards a positive pole, it causes an upward deflection on the ECG and vice versa.

*Plane* refers to a cross-sectional view of electrical activity in the heart. For example the frontal plane provides an anterior-to-posterior view of electrical activity.

### **2.3.1 The 12-Lead ECG System**

The 12-lead ECG consists of 12 leads that are placed on the limbs and chest. These 12 leads provide 12 different views of the heart's electrical activity.

The six limb leads - I, II, III, augmented vector right (aVR), augmented vector left (aVL), and augmented vector foot (aVF)- provide information about the heart's

vertical plane. The augmented leads are unipolar while the other three limb leads are bipolar.

The six chest, or precordial leads - V1, V2, V3, V4, V5, and V6 - provide information about electrical activity in the heart's horizontal plane. The precordial leads are unipolar just like the augmented limb leads. These unipolar leads have another indifferent electrode at the center of the heart.

### 2.3.1.1 Limb Leads

Figure 2-3 shows the placement of the limb leads where LL refers to the left leg. The three bipolar limb leads form the basis of Einthoven's Triangle. The augmented limb leads are derived from the same three electrodes as in leads I, II, III. A brief explanation follows:

- Lead I is bipolar with positive electrode on the left arm and negative electrode on the right arm.
- Lead II is bipolar with positive electrode on the left leg and negative electrode on the left arm.
- Lead III is bipolar with positive electrode on the left leg and negative electrode on the right arm.
- Lead aVR has the positive electrode on the right arm. The negative electrode is a combination of the left arm and leg electrodes.
- Lead aVL has the positive electrode on the left arm and the negative electrode is a combination of the right arm and left leg electrodes.
- Lead aVF has the positive electrode on the left leg while the negative electrode is a combination of the right arm and left leg electrodes.

Together these leads form the "hexaxial" reference system. The hexaxial reference system is used to determine the heart's electrical axis in the vertical plane. The term *electrical axis* refers to the general direction of the heart's depolarization wavefront [3].

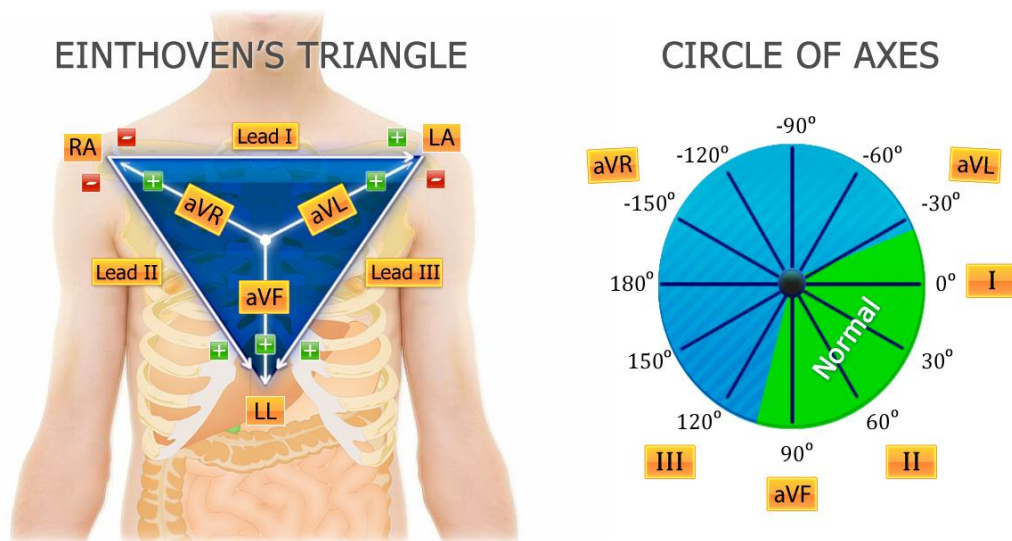


Figure 2-3 Limb lead placement [3]

### 2.3.1.2 Precordial Leads

The precordial leads are placed in a sequence across the chest. They provide a view of the heart's horizontal plane. The six electrodes are considered positive and a negative reference is calculated. Figure 2-4 shows the placement of the precordial leads.

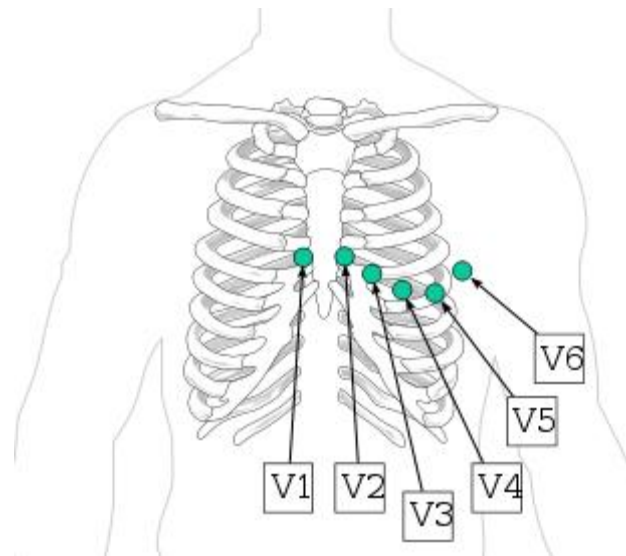


Figure 2-4 Precordial lead placement [3]

### 2.3.2 Three Electrode ECG System:

The system used for ECG acquisition in this project is similar to lead I of the limb leads with an additional right leg drive. The right leg drive is used to remove electromagnetic interference and provides a reference point for the ECG signal. Since we are only using one of the leads, the ECG signal obtained will only provide information about the heart's electrical activity from perspective of lead I. The acquisition system has been described in a later section.

## 2.4 ECG Waveform

This section describes a typical ECG waveform and its various components. Figure 2-5 shows a typical ECG waveform. The baseline voltage of the ECG is known as the isoelectric line. A discussion of the components follows.

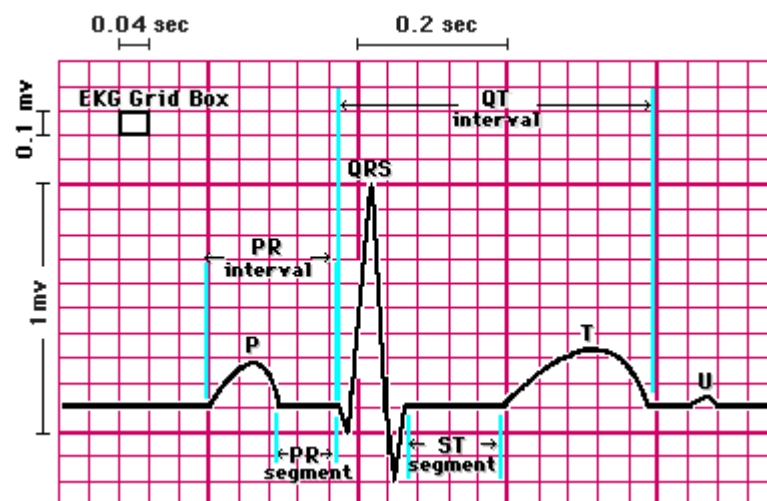


Figure 2-5 ECG waveform [3]

### 2.4.1 P Wave

The P wave is the first component of the ECG waveform and represents atrial depolarization. The P wave is usually seen upright in lead I (which we are using). If the deflection of the P wave is normal and the P wave precedes the QRS complex, this means that the electrical activity originated in the SA node. A normal P wave is 0.06 to 0.12 seconds in duration [3]. The relationship between P waves and QRS complexes allows us to distinguish between various cardiac arrhythmias.

### **2.4.2 QRS Complex**

The QRS complex represents the depolarization of the ventricles and follows the P wave. The depolarization of the ventricles causes them to contract and pump blood through the arteries. The QRS complex looks “spiked” since the Bundle of His and Purkinje fibers coordinate the depolarization of the ventricles leading to an increase in conduction velocity. A normal QRS complex is 0.06 to 0.10 seconds in duration [3].

The Q wave is generally represented by the first negative deflection after the P wave, the R wave is represented by the first positive deflection after the Q or P wave, and the S wave is represented by the first negative deflection after the R wave. The QRS usually appears upright in lead I. Every QRS complex may not contain a Q wave, an R wave, and an S wave. A missing QRS complex may indicate AV block while deep and wide Q waves may represent myocardial infarction.

### **2.4.3 T Wave**

The T wave represents the repolarization of the ventricles. The T wave is usually upright in lead I. The period from the beginning of QRS complex to the apex of the T wave is known as the absolute refractory period. The last half of the T wave is called the relative refractory period. During the relative refractory period the cells are vulnerable to extra stimuli and a bump in the T wave may indicate that a P wave is hidden in it. Tall or peaked T waves might indicate myocardial injury while inverted T waves may represent myocardial ischemia [3].

### **2.4.4 U Wave**

The U wave is not always visible on the ECG. It represents the repolarization of the Purkinje fibers. A prominent U wave may be due to hypercalcemia or hypokalemia, among other causes.

### **2.4.5 PR Interval**

The PR interval represents the movement of the atrial impulse through the AV node, Bundle of His and the right and left bundle branches.

Short PR intervals may indicate the impulse did not originate at the SA node. Prolonged PR intervals may represent a conduction delay through the AV node due to conduction tissue disease, ischemia, heart block etc.



### ***2.4.6 QT Interval***

The QT interval measures ventricular depolarization and repolarization and is around 0.40 seconds in duration [3]. The length of the QT interval varies according to the heart rate. The faster the heart rate the shorter the QT interval.

### ***2.4.7 ST Segment***

The ST segment represents the end of ventricular depolarization and the start of the ventricular repolarization. The ST segment starts at the J point, the junction between the QRS complex and the ST segment, and ends at the start of the T wave. The ST segment is typically 0.08 to 0.12 seconds long [3]. A depressed ST segment may indicate myocardial ischemia. ST segment elevation may indicate myocardial infarction.

## 3 ECG Acquisition

This chapter describes ECG acquisition: techniques to acquire an ECG and the different parts of the acquisition circuit.

### 3.1 Basic Concept

ECG acquisition circuit can be divided into following parts as in Figure 3-1.

- 1) Electrodes
- 2) Instrumentation amplifier
- 3) Filtering to remove noise

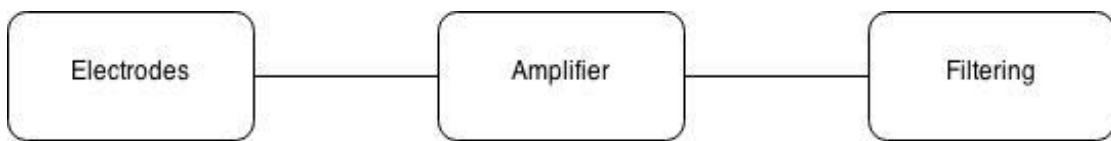


Figure 3-1 Block Diagram of ECG Acquisition Circuit

#### 3.1.1 Electrodes

An amplifier usually has high input impedance and ideally the input current is zero. However a non-zero current flows from the bio potential electrode to input of the amplifier. In human body current is carried out by ions. While in the wires connecting the electrodes to the amplifier, the current is carried out by electrons. A transducer, represented by ECG electrodes in the circuit, is used for the interface between the body (ionic current) and the amplifier circuit (electronic current).

##### 3.1.1.1 Electrode Groups

Ideally bio potential electrodes have two groups. In non-polarizable electrode current flows freely across the electrode-electrolyte interface. These electrodes behave as resistors as in Figure 3-2

Polarizable electrodes have no transfer of charge between electrode-electrolyte interfaces. These electrodes behave as capacitors as shown in Figure 3-3 [4]. The current that flows is displacement current. Practical electrodes have characteristics in-between polarizable and non-polarizable electrodes as neither of the two can be fabricated.

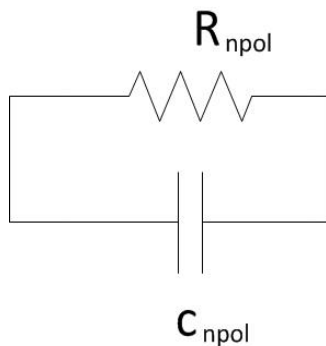


**Figure 3-3 Non Polarizable Electrode**

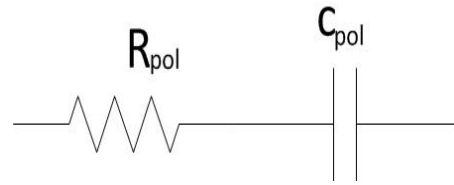


**Figure 3-2 Polarizable Electrode**

### **3.1.2 Electrode Types**

There are three types of electrodes. A brief discussion of each follows.

*Dry electrodes* do not use gel to make conducting path between surface of skin and electrode. Due to lack of electrolyte their characteristics resemble those of polarizable electrodes.

*Non-contact electrodes* use remote sensing of bio potential. These are safe as no current is drawn from the body. To extract bio potential signal from non-contact electrode, the input impedance of the amplifier should be very high.

*Wet electrodes* use gel as electrolyte between skin and the electrode. Their characteristics approach those of non-polarizable electrodes. The most commonly used type is Ag/AgCl (silver-silver chloride) electrode. The gel is used to conduct current between electrode and skin surface. In our project we used wet electrodes as these electrodes are cheap and can be used with long connecting wires due to their low impedance.

### **3.1.3 Amplifier**

The basic purpose of a bio amplifier is to amplify an extremely weak signal. The greatest challenge is to extract a weak bio potential signal (.5 mV-5 mV) [5]. For long term power autonomy of circuit, power dissipation of amplifier has to be minimized. Furthermore signal obtained by electrode is coupled with DC signal of up to 300mV [5].

### 3.1.3.1 Instrumentation Amplifier

The wires connected to the electrodes are directly connected to the instrumentation amplifier. A highly sensitive instrumentation amplifier is used, as ECG signal is in millivolts. The instrumentation amplifier should amplify ECG signal while attenuating common mode signals. Common mode rejection ratio (CMRR) defines the ability of the instrumentation amplifier to reject voltages common to both inputs. Only the differential input is amplified. The most popular topology of the instrumentation amplifier is the three op-amp topology shown in Figure 3-4 [6].

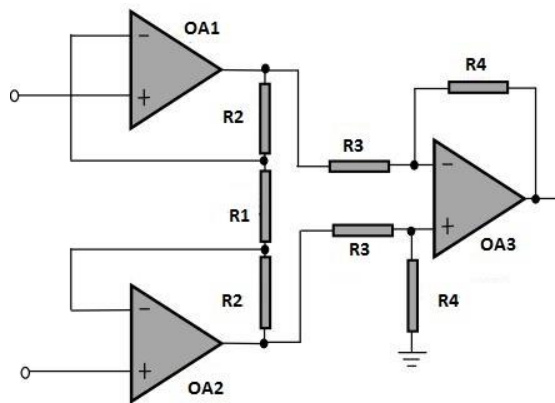


**Figure 3-4 Three Operational Amplifier Differential Amplifier Topology [6]**

Operational amplifier OA1 and OA2 provide infinite input impedance while amplifying differential input. The common mode gain  $A_c$  and differential gain  $A_d$  are given by equation 3.1 and 3.2.

$$A_d = \left( \frac{1}{2} + \frac{R_2}{R_1} \right) \left( \frac{R_{4,top}}{R_{3,top}} + \frac{R_{4,top}}{R_{3,top}} \left( \frac{R_{4,bottom}}{R_{3,bottom} + R_{4,bottom}} \right) + \frac{R_{4,bottom}}{R_{3,bottom} + R_{4,bottom}} \right) \quad (3.1)$$

$$A_c = \left( 1 + \frac{R_{4,top}}{R_{3,top}} \right) \left( \frac{R_{4,bottom}}{R_{3,bottom} + R_{4,bottom}} \right) - \left( \frac{R_{4,top}}{R_{3,top}} \right) \quad (3.2)$$

While using discrete component implementation of the instrumentation amplifier, optimal performance in term of high common mode rejection ratio (CMRR), stability, and differential gain are difficult to compute. In discrete component implementation it is important to have accurately matched resistors. The slightest error in resistor  $R_{3,top}$ ,  $R_{3,bottom}$ , and  $R_{4,top}$ ,  $R_{4,bottom}$  results in unwanted common mode amplification.

The three op-amp topology of instrumentation amplifier is available as an integrated circuit. Integrated instrumentation amplifiers, such as AD620, vastly outperform their discrete component implementation. AD620 draws maximum of 1.3mA supply current [7]. An op-amp such as LF353 draws 6.5mA per chip [8]. AD620 was chosen since it is cheap and is available in the market. The gain of AD620 is controlled by a single external resistor. The gain is given by equation 3.3.

$$Gain = 1 + \frac{49.9k\Omega}{R_G} \quad (3.3)$$

### **3.1.4 Filtering**

To talk about filtration we must first be acquainted with the common sources of noise that can degrade the ECG.

#### **3.1.4.1 Noise**

There are many sources of noise that affect the ECG such as electromagnetic interference (EMI), noise due to muscle movement, radio interference etc. We have only worked on removing EMI since it is a major source of noise.

Electromagnetic interference causes a lot of problem in acquiring ECG. Electromagnetic interference is caused by the magnetic field produced by current carrying conductors. When this magnetic field cuts the loop made by human body, electrode lead and amplifier, it produces electromagnetic interference. The power component of line frequency is very high and it overpowers the ECG signal since the ECG signal is a low frequency signals (0-150 Hz) [4] and its power is small. Line interference can be minimized by decreasing the length of wires connecting the electrodes and the amplifier, implementing a filter, using a Faraday cage etc.

### 3.1.4.2 Low Pass Filter

The output of instrumentation amplifier is band limited by a low pass filter. A Low pass filter is required because the output of instrumentation amplifier still has a large component of line frequency. Simple RC passive low pass filter was used for filtering purpose.

## 3.2 ECG Acquisition System

The ECG acquisition system that was used has three electrodes. Two electrodes are used to acquire the ECG signal (Right arm and Left arm). The third electrode provides a reference for the ECG signal. The system can be divided in the following parts as shown in Figure 3-5.

1. Instrumentation amplifier
2. Right leg drive
3. Filtering

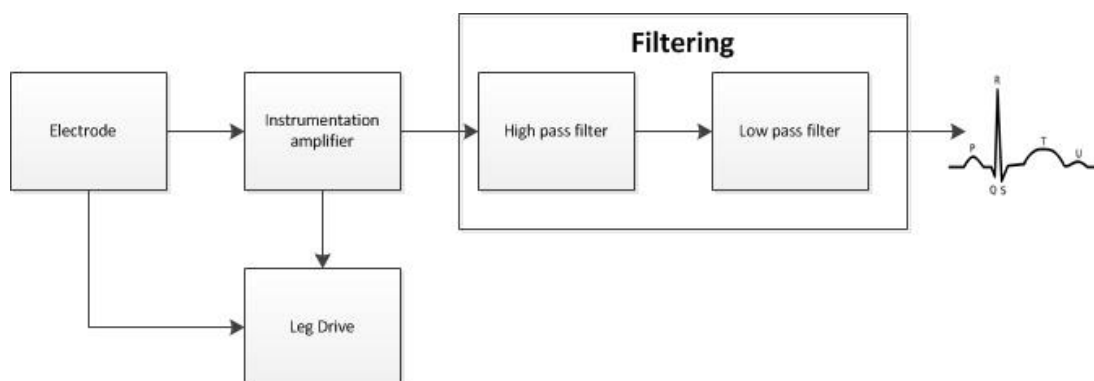


Figure 3-5 Block Diagram of three Lead ECG system

### 3.2.1 Instrumentation Amplifier

The instrumentation amplifier used to amplify differential input was AD620. The connection scheme used has been shown in Figure 3-6 [5]. The right leg drive was connected between two 22kΩ resistors. These resistors were used so that the gain of AD620 can easily be changed by changing  $R_G$ . These resistors also provide a constant gain to the right leg drive. This configuration changes the gain formula of AD620 and now it is given by equation 3.4.

$$Gain = 1 + \frac{49.9k\Omega}{R_G} + \frac{49.9k\Omega}{2 * 22k\Omega} \quad (3.4)$$

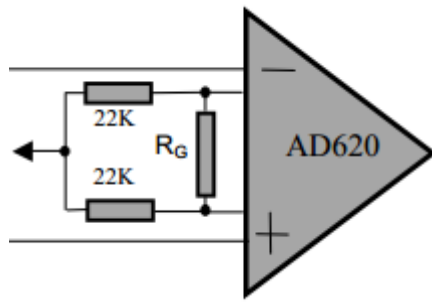


Figure 3-6 AD620 Circuit [5]

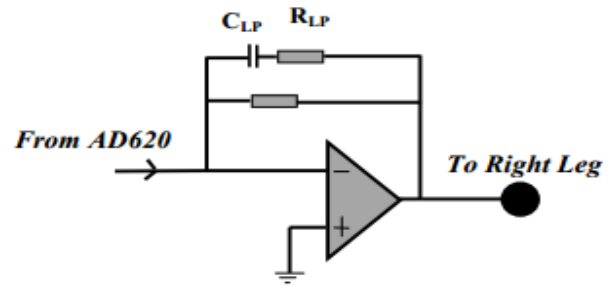


Figure 3-7 Leg Drive

The maximum gain of AD620 is 10,000 [7]. Ideally we would select the maximum possible gain but the gain has to be selected keeping in mind that the output does not saturate. Initially the gain was set to 10. After practical implementation the gain was increased and the final gain of circuit was 100 i.e.  $R_G=500\Omega$ .

### 3.2.2 Right Leg Drive

The right leg drive injects an inverted version of the common mode signal into the patient. This reduces the common mode signal at the inputs of AD620. The operational amplifier used for this circuit was LF353. This circuit, shown in Figure 3-7, act as a low pass filter with cut off frequency of 160 Hz ( $C_{LP}=100\text{nF}$ ,  $R_{LP}=10\text{k}\Omega$ ).

### 3.2.3 Filtering

To band Limit the signal low pass and high pass filters were used. Low pass filter was used to band limit the signal and to decrease the power component of 50 Hz frequency. We used simple RC low pass filter with cut off frequency of 35 Hz as shown in Figure 3-8. To provide high roll off, two low pass filters were connected in series. High pass filter was used to remove DC offset present in ECG waveform. High pass filter with cutoff frequency of 0.5 Hz was designed ( $R1 = 4.5 \text{ k}\Omega$ ,  $R2 = 45\text{k}\Omega$ ,  $R3 = 6.8 \text{ k}\Omega$ ,  $C3 = 1 \mu\text{F}$ ,  $C4 = 0.1 \mu\text{F}$ ,  $C5 = 47 \mu\text{F}$ ).

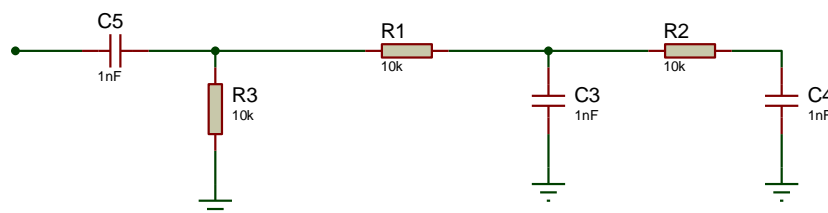


Figure 3-8 High pass and Low pass Filters

## 4 Interfacing

The last part of a data acquisition is concerned with making the analog ECG signal available to a computer for further processing. From the various options available to us for interfacing like serial bus, parallel bus, universal serial bus (USB), sound card of PC, etc., we decided to choose,

- 1) Universal serial bus (USB)
- 2) Sound card of the PC

The original aim was to use USB but as an alternative, sound card of PC was also used as a contingency plan. This was needed since the implementation of a USB interface is a difficult task while interfacing with the sound card is relatively easier.

### 4.1 Interfacing using USB

The overall scheme of interfacing using USB is shown below in Figure 4-1.

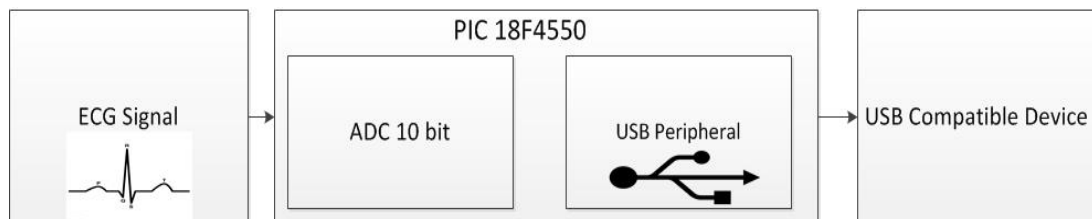


**Figure 4-1 Block Diagram for USB interface**

The analog ECG signal is converted into digital (binary) form using 10-bit analog to digital converter (ADC) of the microcontroller PIC18F4550. The microcontroller also has a USB module in it, which is used to transmit the output of analog to digital converter (ADC) to a USB compatible device like PC for further processing and analysis.

#### 4.1.1 Analog to Digital Converter (ADC)

Analog to digital converter (ADC) is a device that is used convert an input analog signal into a set of digital (binary) values. We used the onboard ADC of PIC18F4550 for analog to digital conversion. PIC18F4550 has a 10-bit ADC which means that the voltage level of any input signal will be divided into  $2^{10} = 1024$  steps.



The reference voltage together with the resolution of analog to digital converter (ADC) dictates the step size. PIC18F4550 provides us with the flexibility to set the step size by providing provision for both positive and negative reference voltages. Since the amplitude of ECG signal was limited to  $\pm 1$ Volts peak, we used +1Volt for positive reference and -1Volt for negative reference. Hence the step size in our case came out to be 1.95 mV as given in equation 4.1.

$$\text{Step size} = \frac{V_{ref(+)} - V_{ref(-)}}{2^n} = \frac{1 - (-1)}{2^{10}} = 1.953125mV \quad (4.1)$$

Acquisition time, is the time taken by the charge holding capacitor to fully charge to the input channel voltage level. For PIC18F4550 analog to digital converter acquisition time was calculated to be,

$$\text{Acq. time} = (0.2 + 0.572)\mu s = 0.772\mu s$$

We have considered the temperature to be less than  $25^\circ\text{C}$ , therefore  $T_{\text{coff}}=0\mu s$  as described in the datasheet [9]. For details on configuration of the ADC, refer to Appendix A.

#### **4.1.2 Universal Serial Bus (USB)**

The microcontroller PIC18F4550 has a built in USB serial interface engine (SIE) that supports full (12Mbps) and low (1.5Mbps) speed communication between any USB host and microcontroller. The SIE can be interfaced directly to the USB using the internal transceiver of the microcontroller. The power to the internal transceiver can be provided by enabling the 3.3V internal regulator and full or low speed mode for communication with the host can be selected [9].

The speed of the device on the bus is set by connecting a  $1.5k\Omega \pm 20\%$  resistor between 3.3Volts line ( $V_{\text{USB}}$ ) and either of the two data lines (D+ or D-) at the device end. For a full speed bus the resistor is connected to D+ line while for a low speed bus the resistor is connected to D- line. In PIC18F4550 internal pull up resistors can be used to set the device in full speed mode on the bus.

#### **4.1.2.1 USB bus communication**

There are four ways for the transmission of data on the universal serial bus [10].

- 1) Isochronous
- 2) Bulk
- 3) Interrupt
- 4) Control

We used interrupt mode of transfer for the transmission of ECG data to the PC because it ensures data integrity timeliness of delivery.

#### **4.1.2.2 Implementation of USB interface using PIC18F4550**

From the data sheet of PIC18F4550 we can see that PORTC pins RC4 (pin23) and RC5 (pin 24) are used for USB interface. RC4 is USB data D- pin and RC5 is USB data D+ pin. Internal pull up resistors were used to configure the device in full speed mode (12Mbps). The overall operation of the USB module of microcontroller is controlled by three control registers and a total of twenty two registers to manage the actual USB transactions. Instead of configuring these registers we used MikroC library functions to implement USB transactions.

When a USB device is plugged into the bus, the process of enumeration begins. In MikroC IDE we added a descriptor file which takes care of the process of enumeration. This file was created using HID terminal of the MikroC IDE. Configuration bits for the microcontroller were set by editing the project settings in MikroC IDE.

The working of the code written in C to convert the analog ECG signal to digital form and transmit the output of analog to digital converter (ADC) to a PC using USB can be understood from the flow chart shown in the Figure 4-2. The code for conversion is present in Appendix C.

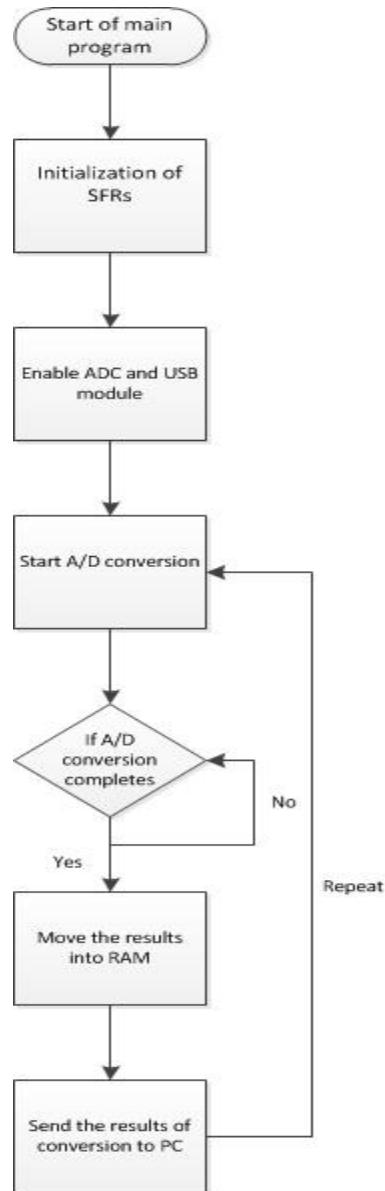


**Figure 4-2 Flow chart**

### ***4.1.3 USB Compatible Device***

A routine in Python was written to acquire the digital ECG data, on computer, sent by the microcontroller. The overall operation of the program can be understood from the Figure 4-3,

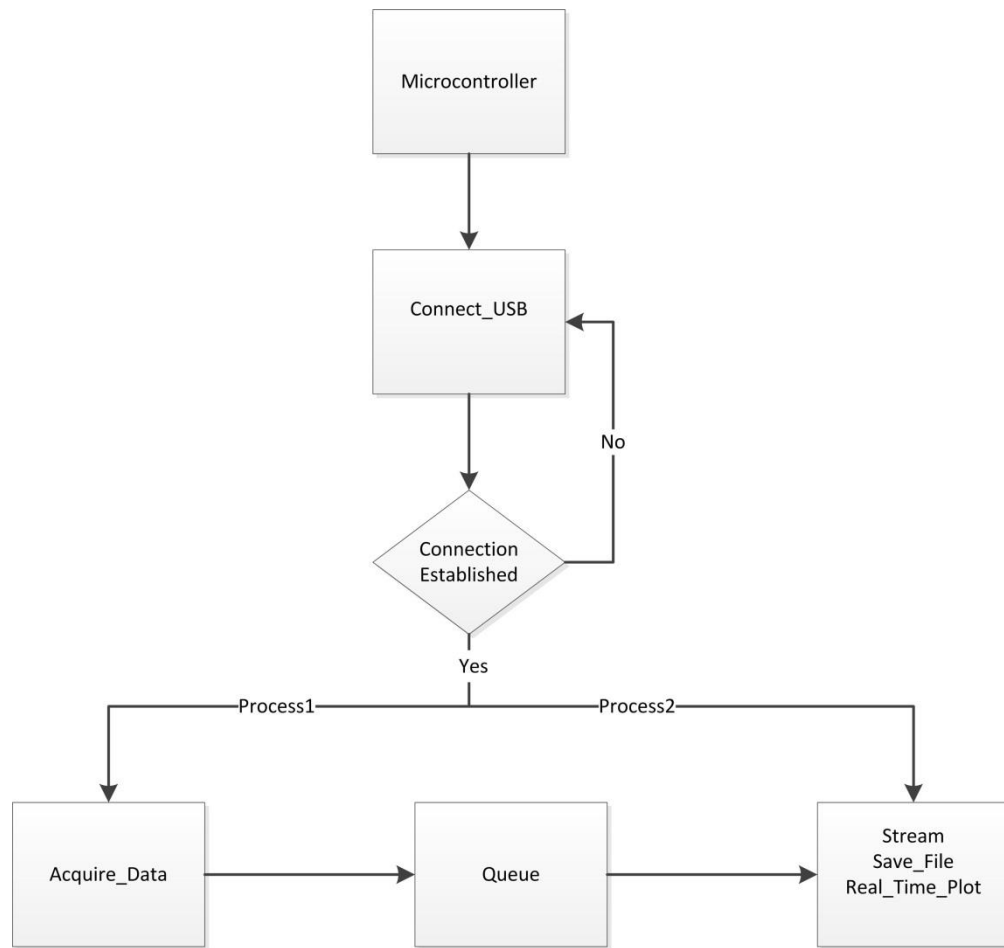


**Figure 4-3 Flow diagram for Main Method**

The method “Connect\_USB” establishes the connection between the microcontroller and the computer. After the connection is established, two processes are initiated which run in parallel. Process1 (Acquire\_Data) takes the ECG data, output by the ADC of microcontroller, and puts it in the queue. Process2 takes the data from the queue and can either save it to a file, stream it to another device or plot it in real time.

The working of the methods “Acquire\_Data”, “Save\_File”, “Stream” and “Real\_Time\_Plot” can be understood from the flow diagrams given in Figure 4-4,

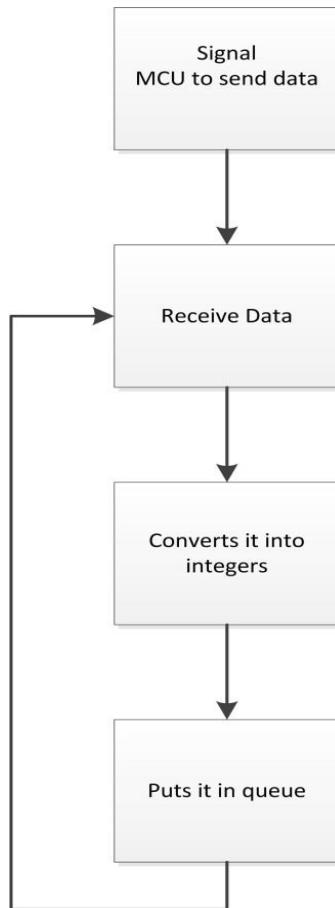


**Figure 4-5 Flow Diagram for the Acquire\_Data Method**

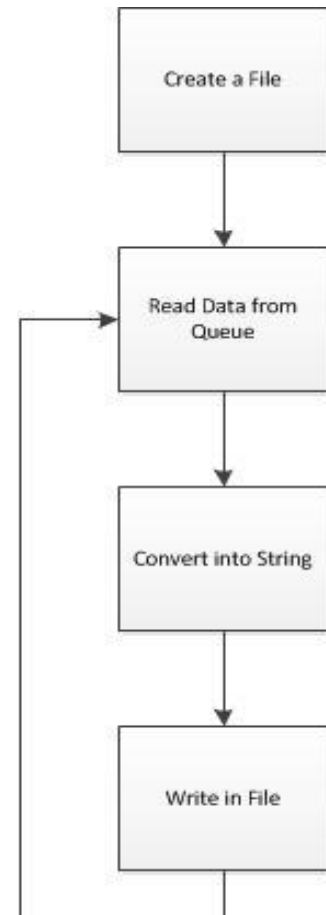


**Figure 4-4 Flow Diagram for the Save\_File Method**

The method Acquire\_Data signals microcontroller to start sending data. The data sent by microcontroller is received and converted into voltages. This data is then sent to the queue. This process is executed in a cycle. A file is opened in writeable mode. Data is read from the Queue and converted into strings. These strings are then written to the file. The process is shown in Figure 4-5.

To stream data a socket must be created on both server and the client. The server socket binds to its own IP address while the client socket connects to the server IP address. A port common to both server and client is used for communication of data. If the connection is established then communication process between server and client starts. Flow diagram is shown in Figure 4-6.

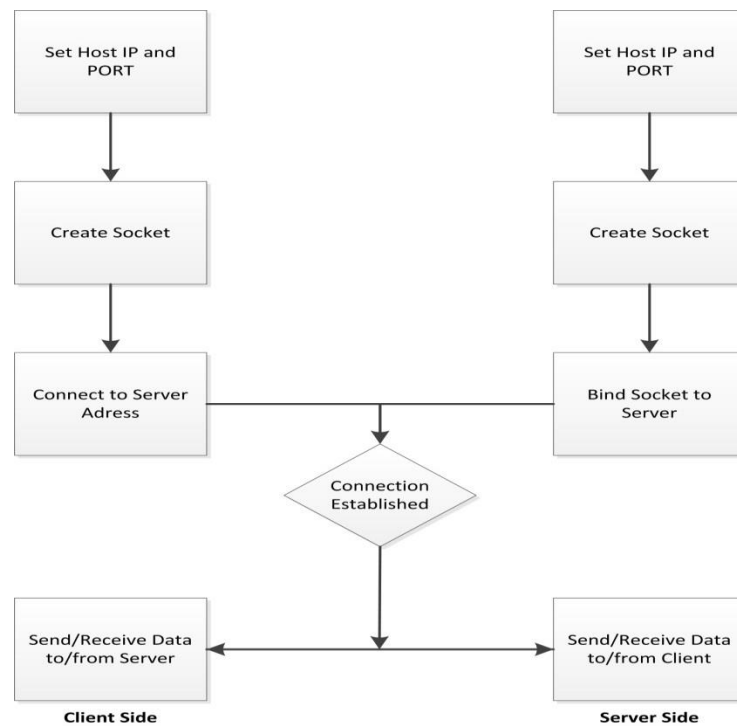


**Figure 4-6 Flow Diagram for the Stream Method**

The Real\_Time\_Plot first creates an empty figure. The data is then read from queue and put in a list. The list is then updated so that only new data is plotted. This updated list is then plotted. The code for the complete routine and subroutines along

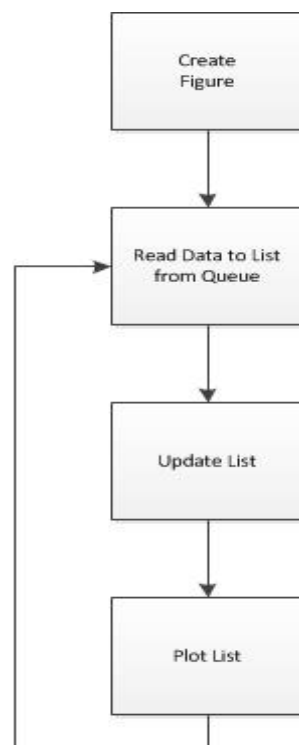


**Figure 4-7 Flow Diagram for the Real\_Time\_Plot Method**

with their documentation is given in Appendix D.

## 4.2 Interfacing using the Sound Card Input

As discussed in the beginning of the chapter, the sound card interface was developed as a contingency plan. The microphone input to a PC, laptop or a smartphone is a ready-made system for data-acquisition since it uses a built-in ADC to sample the input signal. However, the microphone input suffers from at least two problems:

- 1) The input is capacitively coupled.
- 2) The sound card is usually designed to work for a band of frequencies between 20 Hz to 20 kHz.

The major component of an ECG signal lies between 0.5 – 50 Hz [11] . Figure 4-8 shows the input frequency response of a PC sound card to a sine sweep (20 Hz -20 kHz). It can be seen that the roll off starts above 20 Hz in this particular case.

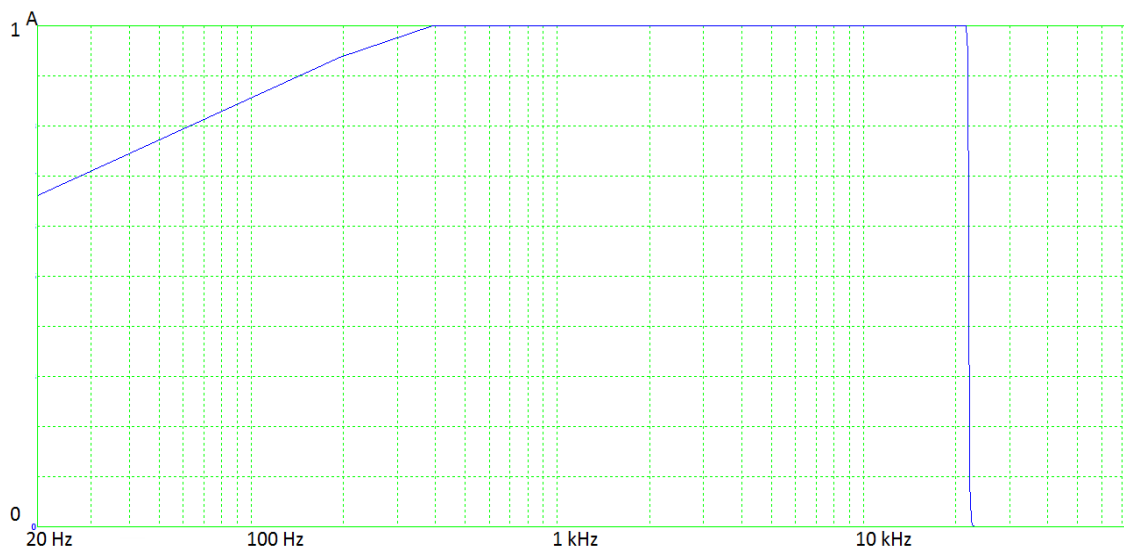


**Figure 4-8 Sound card frequency response**

Most computing devices today have a sound card with a microphone input with at least an 8 bit (usually higher) ADC. However, in order to make use of the sound card for interfacing, the ECG band needs to be shifted to higher frequencies due to the aforementioned problems. This can be readily achieved through Frequency modulation of the ECG signal. Figure 4-9 shows a conceptual diagram of the proposed system

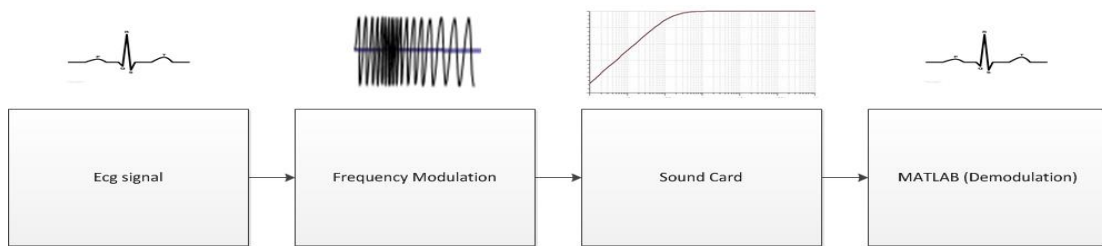


**Figure 4-9 Block Diagram representation of proposed system**

#### **4.1.4 Frequency Modulation**

Frequency modulation allows us to encode the low frequency ECG signal using a high frequency carrier. The frequency of the carrier changes in relation to the amplitude of the ECG signal. A frequency modulated wave can be described by equation 4.2 [12].

$$\varphi_{FM}(t) = A \cos(\omega_c t + k_f \int_{-\infty}^t m(\alpha) d\alpha) \quad (4.2)$$

In equation 4.2,  $\omega_c$  represents the carrier frequency while  $k_f$  is known as the sensitivity. Since FM represents the signal to be transmitted in the variation of the frequency and not the amplitude of the carrier, we can read this frequency modulated signal from the microphone input of the circuit using a software routine. We can also read this signal at the microphone input using MATLAB.

#### **4.1.5 Voltage to Frequency Converter**

Voltage to frequency converters, basically VCOs, are available as integrated circuits and can be used for linear frequency modulation. Another option is to implement a voltage controlled oscillator through various circuit topologies using discrete components. A V to F converter, however, allows the implementation of the modulation scheme using a single IC.

#### **4.1.6 V to F converter design**

Texas instruments LM 331 voltage to frequency converter was selected for frequency modulation since it meets the specifications and is available in the market. Since our



signal can take on both positive and negative voltages, we need a bipolar V to F converter. LM 331 by itself does not allow us to cater to both positive and negative voltage. To this end, the circuit of Figure 4-5 was designed to meet the specifications in Table 4-1. LM331 provides a reference voltage of 1.90V at pin 2. In Figure 4-8 this reference voltage has been used to allow bipolar voltage to frequency conversion.

#### 4.1.6.1 Specifications

**Table 4-1 Design Specifications**

Input voltage range (Vp)	+/- 1V
Sensitivity of VFC	2000 ( $\Delta f = 2 \text{ kHz for } \Delta V_{in} = 1V$ )
Fo (center frequency)	4 kHz
Supply Voltage	9 V (battery)

#### 4.1.6.2 Circuit Diagram:

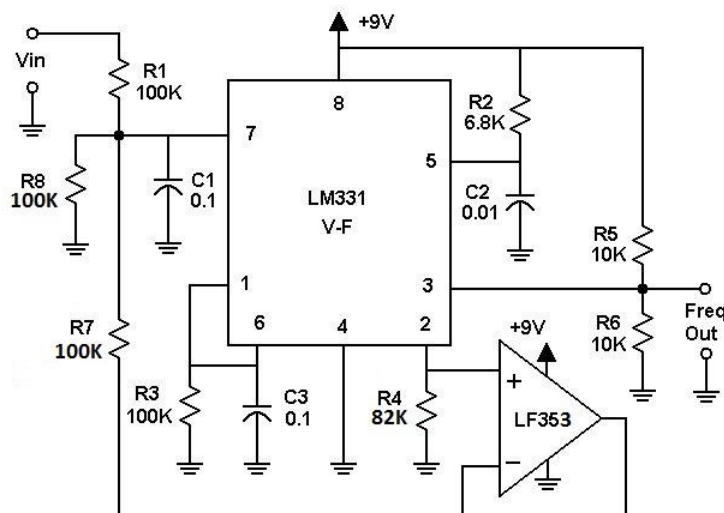


**Figure 4-10 V to F converter circuit [13]**

#### 4.1.6.3 Design:

The design equations are given below [13]. The circuit of Figure 4-10 was designed using these equations to meet the specifications above.

$$F = V7 * \frac{R4}{N} \quad (4.3)$$

Where V7 refers to the voltage at pin 7 and N is given by Eq. 4.4.

$$N = 2.09 * R3 * R2 * C2 \quad (4.4)$$

$$R7 = (Fp - Fo) * 1.9 * \frac{R1}{Fo * Vp} \quad (4.5)$$

$$R4 = N * Fo * \frac{2 * R7 + R1}{1.9 * R1} \quad (4.6)$$

In Eq. 4.5,  $Fp$  refers to the peak frequency of the VFC,  $Fo$  refers to center frequency of VFC ( $V_{in} = 0V$ ) and  $Vp$  is the peak input voltage. For our purposes we chose  $Fo$  to be 4 kHz and  $Fp$  to be 6 kHz which gives a peak negative frequency,  $Fn$ , of 2 kHz.

With these design parameters, we only need to change two resistors,  $R7$  and  $R4$ , to change our input voltage and output frequency range. The output available at pin 3 is a stream of rectangular high-to-low pulses. For more details see [13].

Making use of Eqs.4.5 and 4.6, with the given design specifications, we obtained the following values.

$$R4_{calc} = 86.7 \text{ k}$$

$$R4_{used} = 82 \text{ k}$$

$$R7_{calc} = 95 \text{ k}$$

$$R7_{used} = 100 \text{ k}$$

Since the actual values used were different, a slightly different center frequency of 3.8 kHz was achieved.

#### 4.1.6.4 Testing

The circuit was initially tested by applying DC voltages at pin 7 and observing the output. Table 2 enumerates the results.

**Table 4-2 DC testing of VFC circuit**

Input (mV)	Frequency (kHz)	Input (mV)	Frequency (kHz)
0	3.85	0	3.85
200	4.2	-200	3.4
400	4.6	-400	3
600	5	-600	2.6
800	5.4	-800	2.2
1000	5.8	-1000	1.8

The circuit was then tested by applying time varying voltages of various sorts and observing the output at pin 3.

#### 4.1.7 Interfacing with the sound card

The output at pin 3 is a stream of rectangular pulses of varying widths depending on the input voltage. This output can drive a TTL (logic level: 5V) load [14]. The microphone input of a typical sound card cannot handle such voltages. In order to use the microphone input, we need to scale our FM signal down to a safe level. This was achieved by using a voltage divider (resistive network), and buffering the output in order to isolate the circuit from the microphone input as in Figure 4-8. The output of this circuit can then be safely applied to the line-in of a sound card using a suitable connector (3.5mm jack usually).

The input is to be applied across R2 while the output can be obtained between the nodes labeled output and virtual ground. U1B implements a virtual ground which is used for the reason that LF353 does not work well with a single supply with input voltages close to the supply voltages. Since LF353 comes with two op-amps on a single chip and is readily available, this topology makes sense. U1A implements a voltage follower. The attenuation can be controlled through the potentiometer R2. The ratio actually used was 10: 1 (5V to 0.5V).

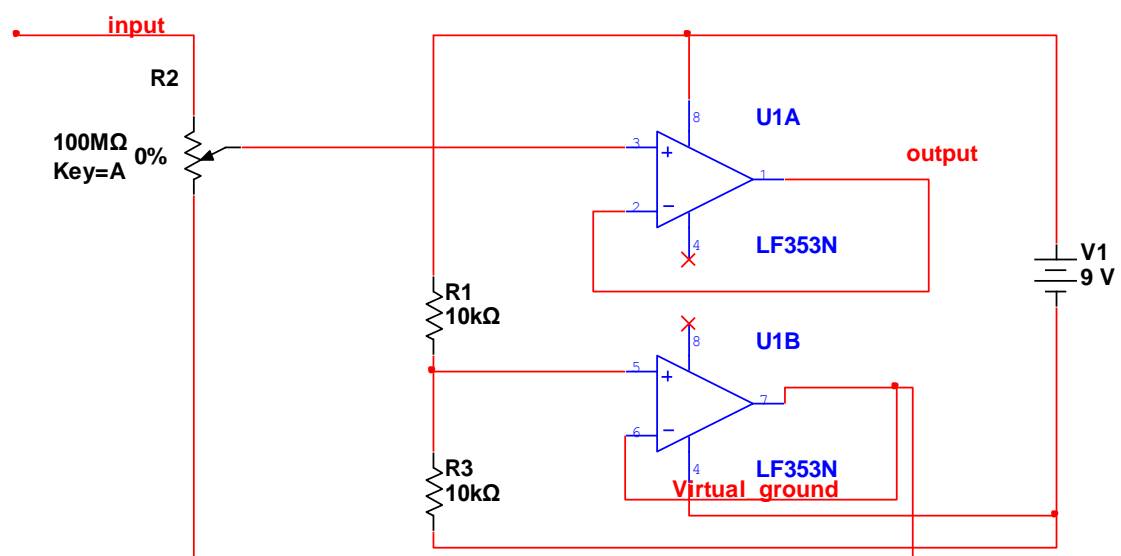


Figure 4-11 Resistive divider

### 4.1.8 Demodulation

The FM signal can be read from the microphone input through MATLAB. MATLAB also provides a built in function to demodulate FM signals. The MATLAB script written for demodulation has been reproduced below.

```
%Set sampling frequency
Fs=44000;
%Create audiorecorder object
y=audiorecorder(Fs,16,1,-1);
%Read into the audiorecorder object from mic-in for 0.5 sec
recordingblock(y,0.5);
%Obtain samples from audiorecorder object
z=getaudiodata(y);
%Plot the signal read at the mic-in
plot(z)
%Demodulate FM with center freq. 3.8 kHz and sensitivity 2000
h=demod(z,3830,Fs,'fm',2000);
%Open new figure window
figure(2)
%Plot demodulated signal in a separate window
plot(h)
```

The demodulated output obtained using this code contained a considerable amount of noise. However, before we could improve the modulating circuitry our USB interface had been implemented and tested to work properly. Work on the sound card interface was thus abandoned.

## 4.2 Acquisition and interfacing circuitry

Figure 4-12 shows the complete acquisition and interfacing circuit developed during the course of this project.

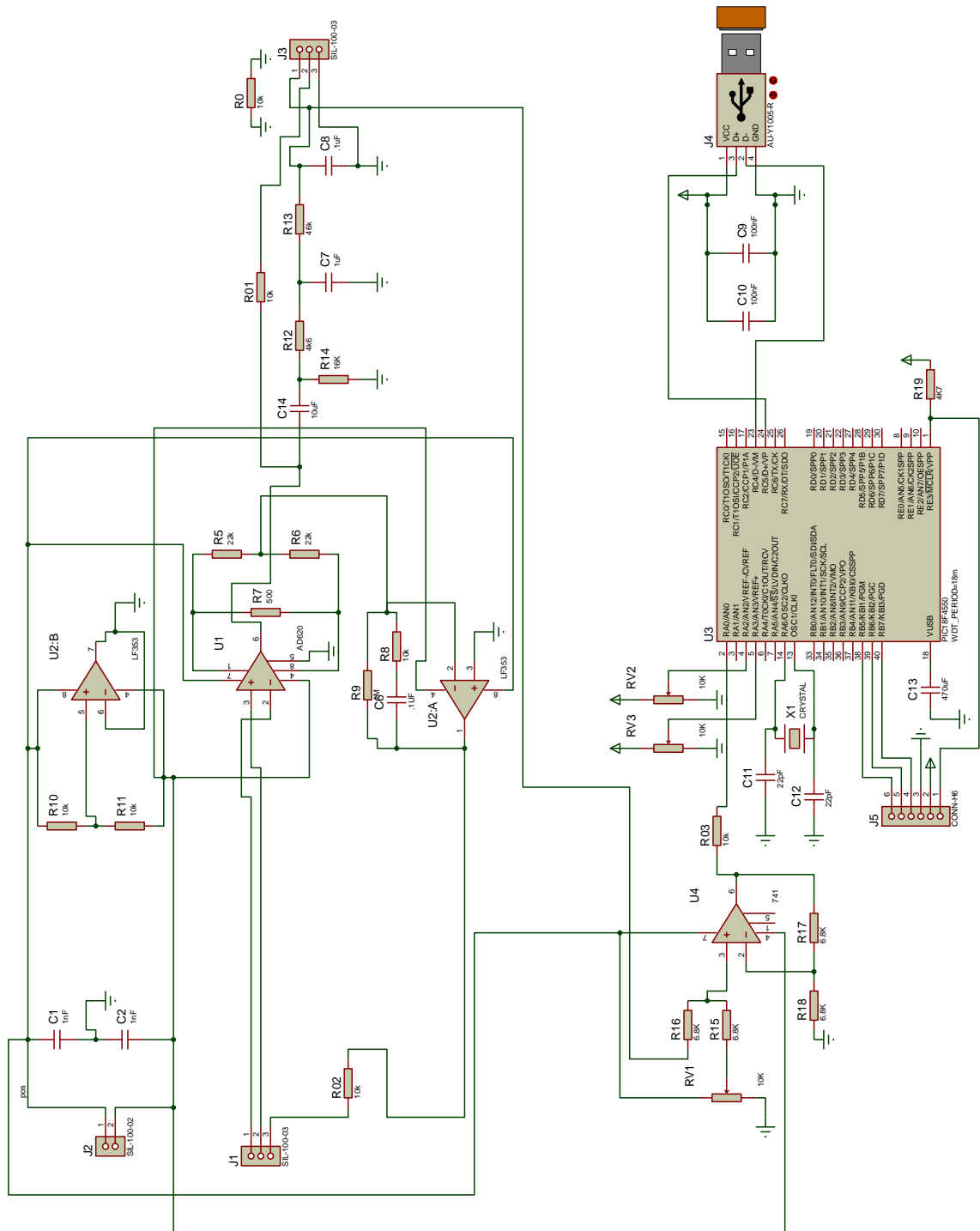


Figure 4-12 Complete circuit

## 5 Artifact Removal and QRS Complex Detection

This chapter presents an overview of artifacts which usually distort an ECG signal and the techniques that were implemented for the removal of these artifacts along with an algorithm for QRS complex detection. These artifacts lower the accuracy of a diagnosis based on such an ECG and therefore their removal is imperative to ensure a reliable diagnosis. Section-1 deals with the artifacts normally present in an ECG and the techniques that were used for their removal. Section-2 presents an algorithm for QRS detection. Section discusses a method to detect R wave peak. The python code for these analyses can be found in Appendix E.

### 5.1 Artifact Removal

This section presents the artifacts that distort the ECG and the techniques used for their removal. For QRS complex detection, the ECG has to be preprocessed in order to remove these artifacts.

#### 5.1.1 ECG Artifacts

The ECG signal is usually corrupted by the following types of artifacts [15] :

1. Power line interference: This presents itself as a 50/60 Hz noise in the ECG. The noise frequency drifts with the change in the power line frequency.
2. Baseline Drift: Baseline drift can usually be attributed to relative motion between the electrode contact surface and the skin and presents itself as a 0.15 – 0.3 Hz signal [16].
3. Quantization noise and aliasing introduced due to digitization of the ECG.

Figure 5-1 shows an ECG signal acquired using our own ECG acquisition system. Baseline drift and noise distorting the ECG is clearly visible. In order to use this ECG for diagnosis we need to remove these artifacts to get a cleaner signal.

#### 5.1.2 Artifact Removal Techniques

This section discusses the techniques implemented for baseline wander and power line interference removal.

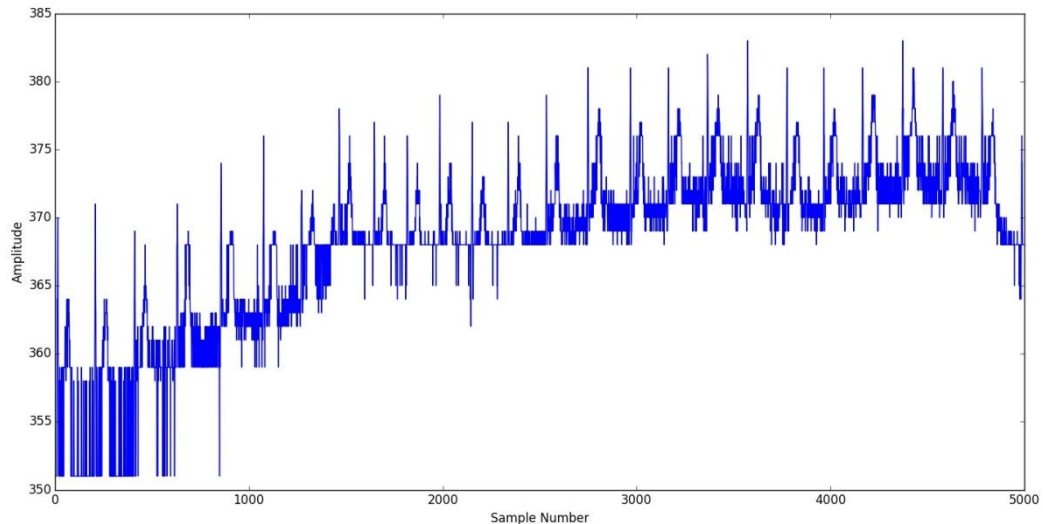


**Figure 5-1 ECG with baseline wander and power line interference**

### 5.1.2.1 Baseline wandering

Baseline wandering can be thought of as a shift in the DC value of the signal and can usually be attributed to relative motion between the electrode contact surface and the skin. Baseline wander has a frequency range 0.05 – 1 Hz [16]. Baseline wander can cause problems in QRS detection and its removal is therefore necessary.

Baseline wander removal techniques can be broadly classified in two categories: polynomial based and filtering based techniques. While polynomial based techniques are more robust, filtering based techniques are easier to implement. A simple high pass filter of cutoff frequency around 0.5 Hz can be used for baseline removal. The high pass filter should have linear phase filter in order to avoid distortion of the ECG.

Linear phase filtering can be achieved by using a finite impulse response (FIR) filter. However FIR filters designed for this purpose are of very high order (700 Hz – 2000 Hz) and cannot be implemented on small datasets due to the delay introduced by FIR filtering. To deal with this problem, infinite impulse response (IIR) forward-backward filtering can be used since an IIR filter with a similar frequency response to an FIR filter usually has a smaller order. Furthermore forward-backward filtering with an IIR filter is equivalent to forward filtering with a filter of squared magnitude and zero phase response [17].

### 5.1.2.2 Power line Interference removal

Power line interference generally presents itself as a 50 or 60 Hz signal added on to the ECG signal. A common method to remove power line interference is to use a digital notch filter to remove frequency components around the power line frequency. However, this does not take into account the drift in the power line frequency and again requires a filter of a very high order due to the small transition band.

Since our main goal is the detection of QRS start and end points we do not need to preserve the entire ECG spectrum. An ECG signal with frequency components in the range 0.5 -45 Hz is adequate for QRS detection [18]. Therefore we can use a low pass digital filter to limit the band of frequency range of the ECG signal below 50 Hz. While this will distort the ECG, the resulting signal would work for our purposes.

### 5.1.3 Implementation and Results

Since baseline wander removal can be achieved using a 0.5 Hz high pass filter while power line interference can be reduced through a 45 Hz low pass filter, a Chebyshev band pass filter of 0.5 – 45 Hz was used for forward backward filtering of the ECG. Figure 5-2 shows the frequency response of the Chebyshev filter designed for this purpose. The order of this bandpass filter is 7 and through forward backward filtering the computational complexity which would have been a problem for say a 500 order FIR filter has been reduced.

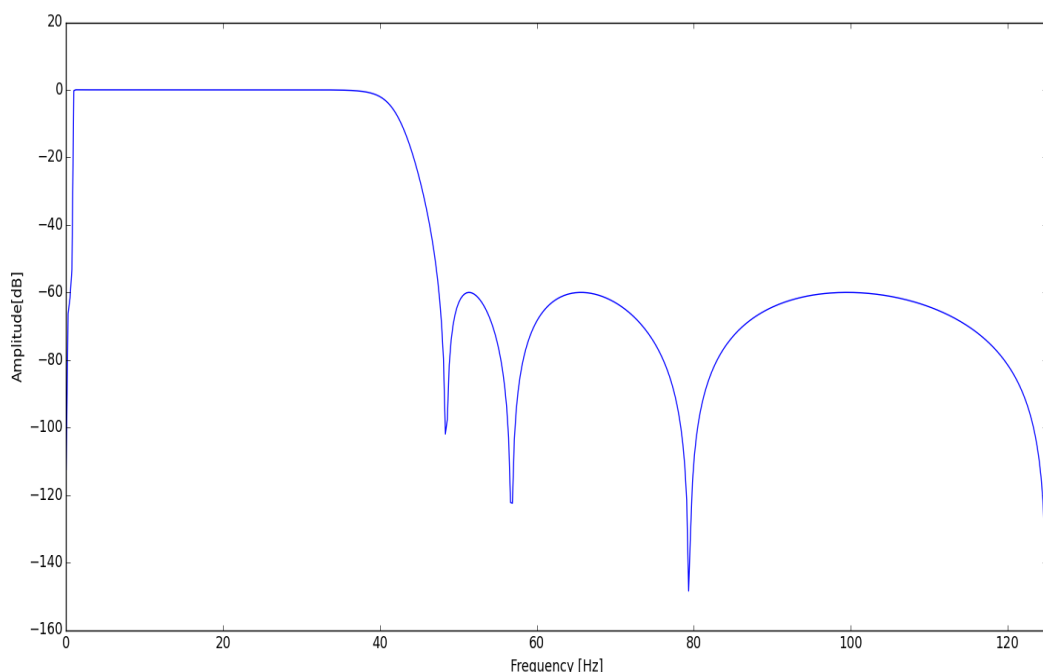


**Figure 5-2 Chebyshev bandpass filter frequency response**



Figure 5-3 compares a raw and bandpass filtered ECG.

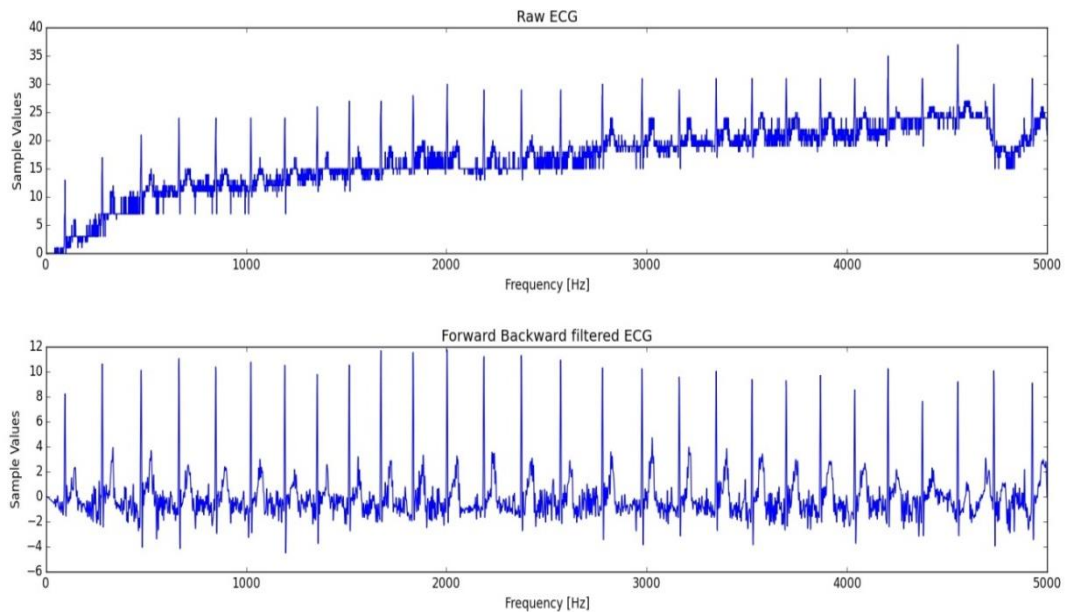


**Figure 5-3 Raw and forward backward bandpass filtered ECG**

## 5.2 QRS detection

As detailed before, the QRS complex represents the depolarization of the ventricles. The detection of the QRS complex is of prime importance in ECG analysis since a fair number of subsequent processing steps are based on this.

### 5.2.1 The Length Transform for QRS detection

We implemented a length transform based algorithm for QRS detection. The algorithm is similar to the popular Pan-Tompkins algorithm. Figure 5-4 presents a block diagram view of the steps involved in QRS complex detection using the length transform algorithm.

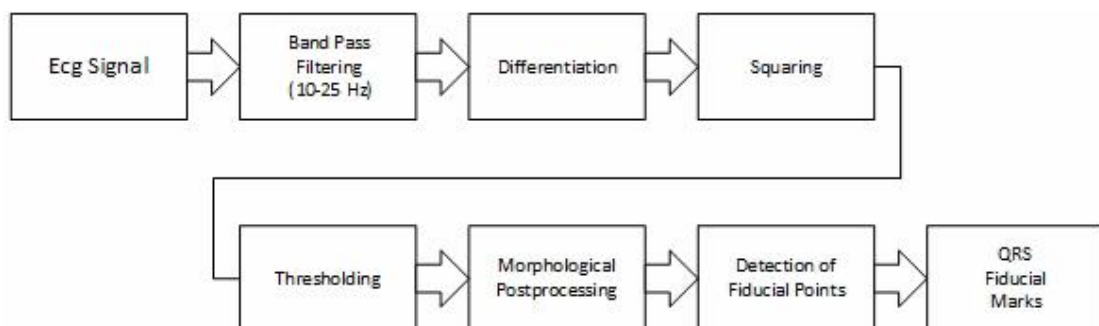


**Figure 5-4 Length transform algorithm for QRS detection**

The algorithm relies on the fact that if we view the ECG signal as being made up of a string, the QRS complexes would consume most of the length of the string i.e. the curve length corresponding to the QRS complex is longer than that of other parts of the ECG. More formally, the curve length corresponding to the QRS complex can be written as in Eq. 4.1. Here  $T_x$  represents the sampling interval and  $y_i$  represents the amplitude of the  $i$ -th ECG sample while  $n$  is the length of the QRS complex in terms of the samples [19].

$$L = \sum_{i=1}^n l_i \sum_{i=1}^n \sqrt{T_x^2 + (y_i - y_{i-1})^2} \quad \text{Eq. 4.1}$$

Eq. 4.1 reduces to Eq. 4.2 if we approximate the length of each hypotenuse ( $l_i$ ) of the triangle with the height. Figure 5-5 illustrates this concept.

$$L = \sum_{i=1}^n D_y \quad \text{Eq. 4.2}$$

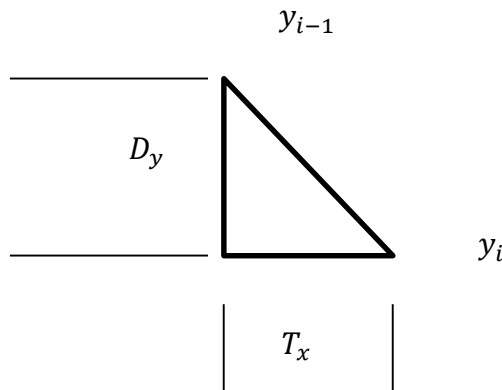


**Figure 5-5 Illustration of the approximation for length transform**

Since  $D_y$  can be negative we will use  $D_y^2$  for the purpose of analysis. Note that  $D_y$  is simply the first order difference of the signal. Since the curve length for QRS complex is generally greater than for any other part of the ECG, this approximation would allow us to identify the QRS complex simply by taking the first order difference of the signal.

### **5.2.2 Implementation and Results**

The implementation of the length transform algorithm for QRS detection follows in the order specified in Figure 5-4.

### 5.2.2.1 Band Pass filtering

The frequency content of the QRS complex lies between 10-25 Hz [18]. A band pass filter designed for this frequency range would remove the low frequency noise attributed to movement or baseline shifts and the high frequency noise, including power line interference, from the ECG. An FIR filter was used for this purpose. Figure 5-6 presents the ECG signal filtered by a band pass (10-25 Hz) filter.

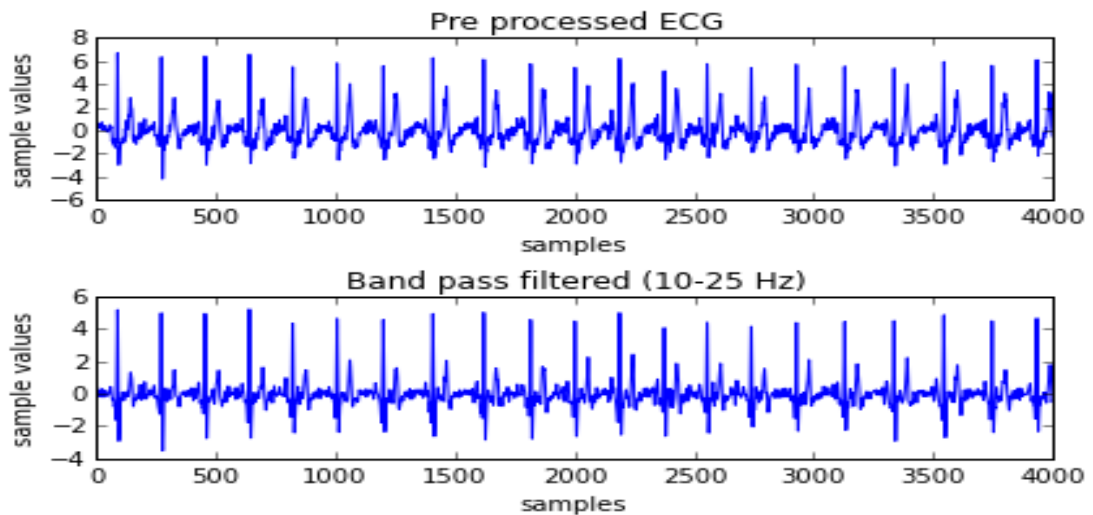


Figure 5-6 The preprocessed ECG filtered by a 10-25 Hz band pass filter

### 5.2.2.2 Differentiation

As discussed before, the curve length of the ECG signal can be approximated by first order difference of the signal. Figure 5-7 compares the band pass filtered and the difference signal. It can be seen that the first order difference has large values for the samples corresponding to the QRS complexes.

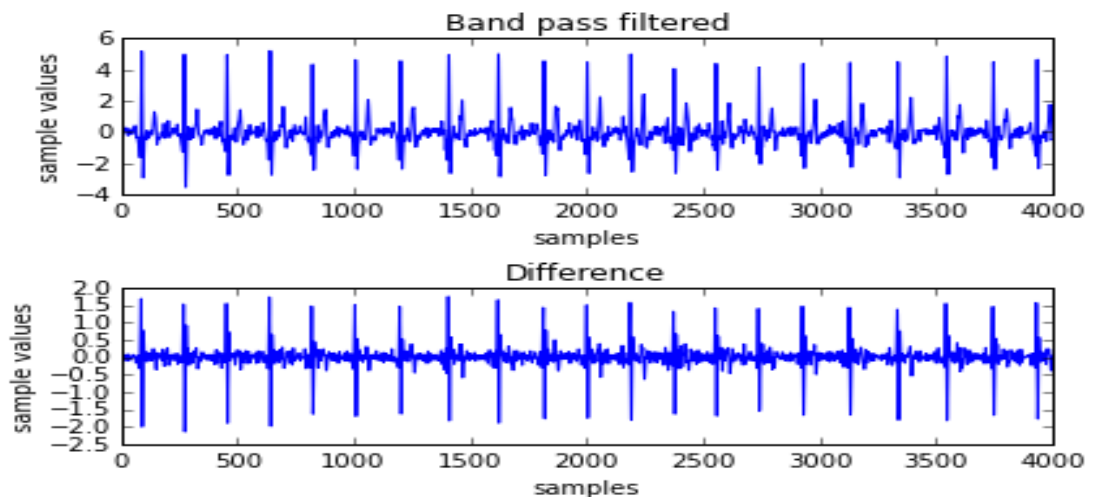


Figure 5-7 First order difference of the band pass filtered signal

### 5.2.2.3 Squaring

The differenced signal is then squared. Figure 5-8 shows the results.

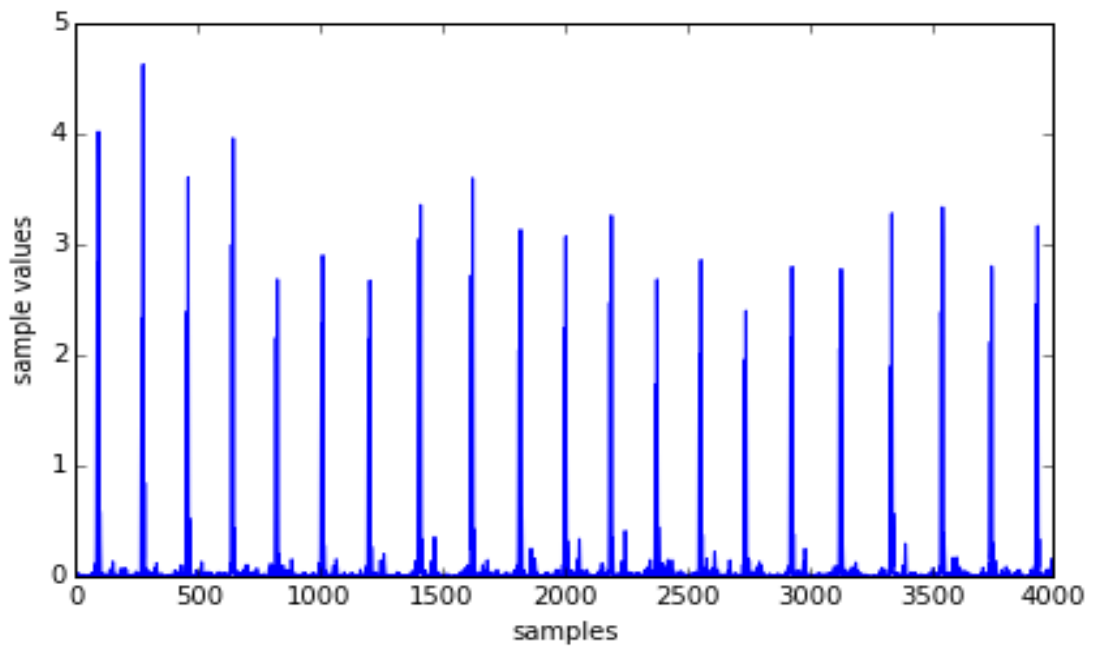


Figure 5-8 Difference squared

### 5.2.2.4 Thresholding

In order to detect the QRS complex, a threshold is defined by averaging the difference squared signal over a window of duration four seconds. A noise factor multiplier is provided to account for the amount of noise in the signal. The samples of the

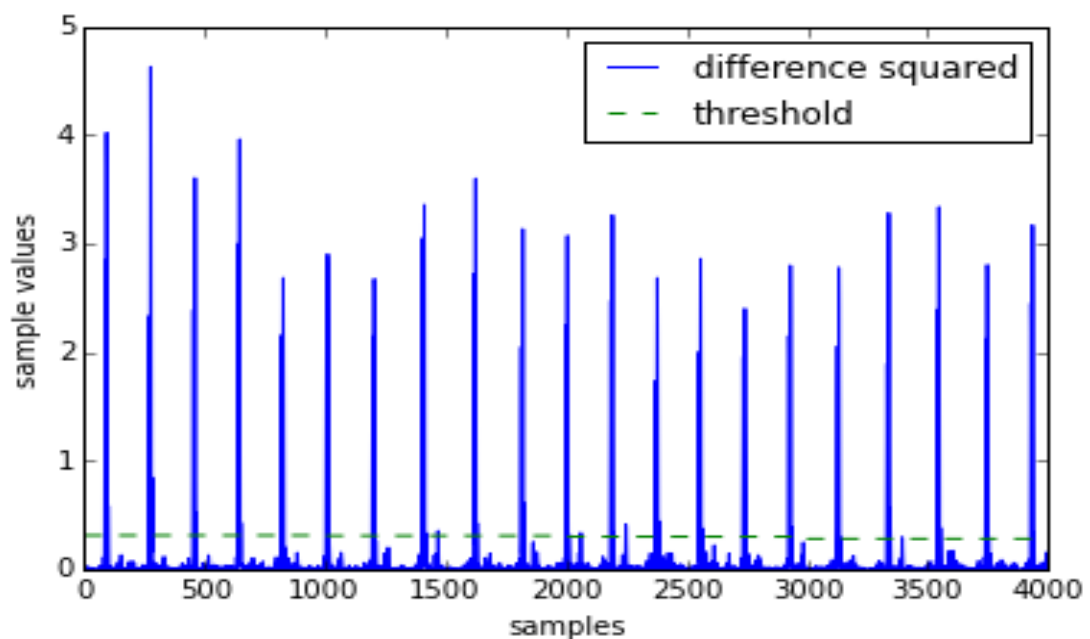
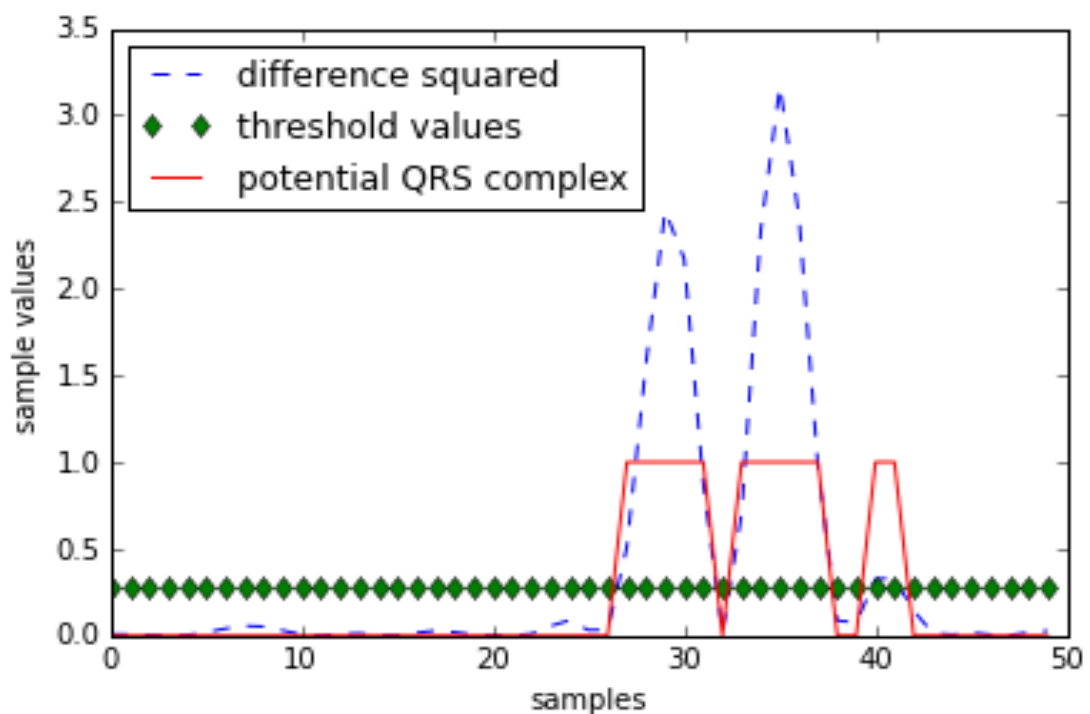


Figure 5-9 Threshold values

difference squared signal greater than the threshold value are marked as potential QRS complexes. Figure 5-8 shows the threshold plotted with the difference squared signal.

Figure 5-10 illustrates the potential QRS complex region obtained through this process. The figure shows the difference squared values obtained for a single QRS complex. In order to detect the actual QRS complex post processing is required to remove the errors (regions erroneously marked as QRS complex) and to detect QRS start and end points since the QRS can be divided into multiple regions as in Figure 5-10.



**Figure 5-10 Thresholding and potential QRS complex region**

#### 5.2.2.5 Morphological post processing

To remove errors and detect QRS start and end points we use morphological opening and closing. Morphological opening is used to remove small spikes in the identified potential QRS complex regions which usually appear due to noise while morphological closing is used to join together potential QRS complex regions if they are close enough. To perform morphological opening, a ones array corresponding to  $0.12 \cdot f_s$  duration (normal QRS length) was used as the structuring element. For morphological closing a ones array corresponding to  $0.04 \cdot f_s$  duration (minimum QRS length) was used as the structuring element. Figure 5-11 illustrates the result of

morphological opening and closing. It can be seen that an isolated spike marked as a potential QRS complex region has been removed (morphological opening) while the spikes which were adjacent have been marked as QRS complex regions (morphological closing).

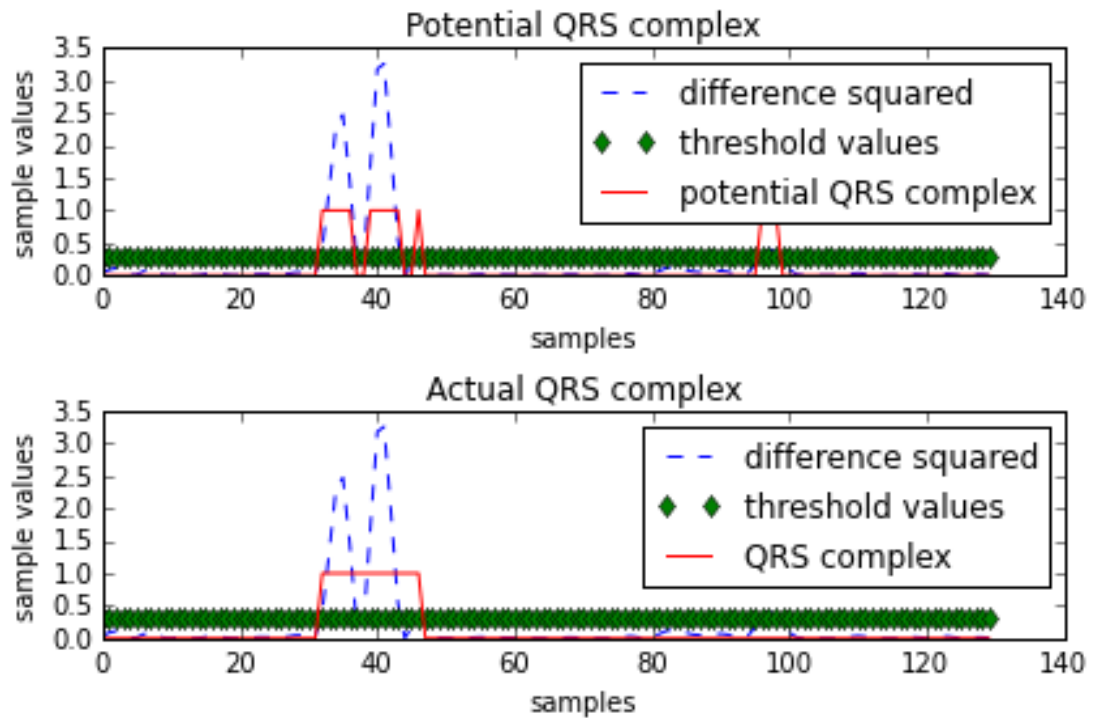


Figure 5-11 Results of morphological opening and closing

#### 5.2.2.6 Detection of QRS fiducial points

Since the regions comprising the QRS complexes are now well defined, a simple difference operation can now be used to find the QRS start and end or fiducial points. Figure 5-12 depicts the results.

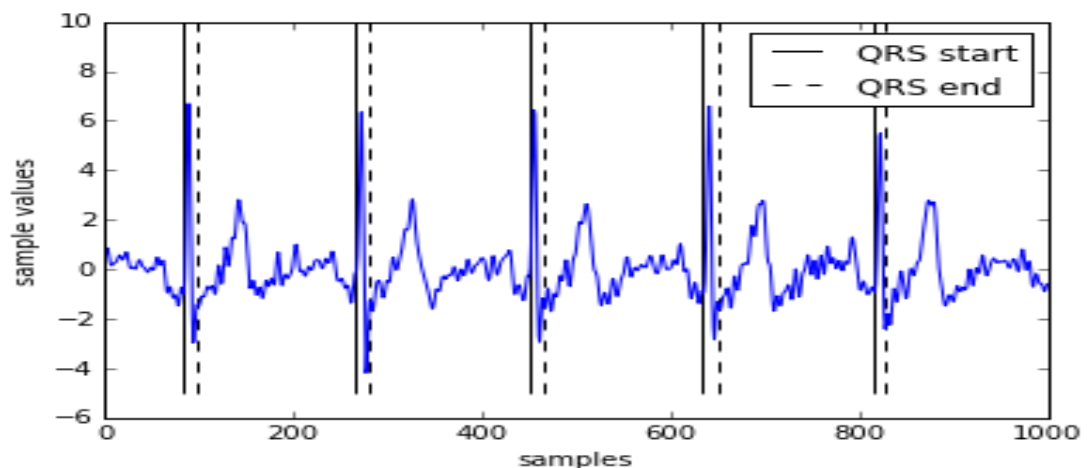


Figure 5-12 QRS fiducial points

### 5.2.2.7 Results

This algorithm is good at detection of the QRS complex but the fiducial points identified by this algorithm need to be further refined to increase the accuracy.

## 5.3 R wave

This section presents a simple method to detect the R peak. Furthermore we present a plot of the running average of the RR-intervals.

### 5.3.1 R peak detection

Since the QRS start and end points have been marked, we use a crude method to approximate the peak of R wave by taking the average of the QRS start and points. This method is not very accurate and is contingent upon the detection of the QRS complex. The R wave peaks approximated by this method have been marked in Figure 5-13.

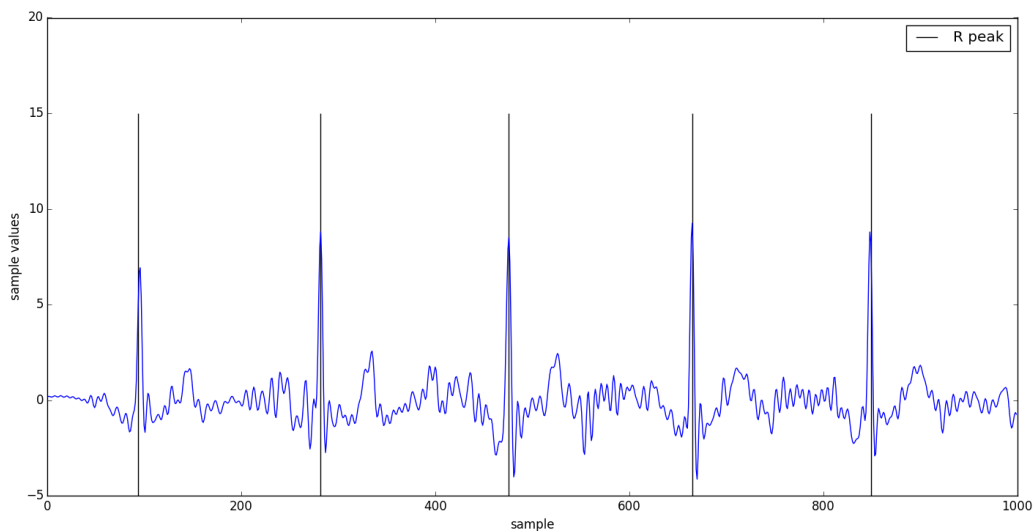
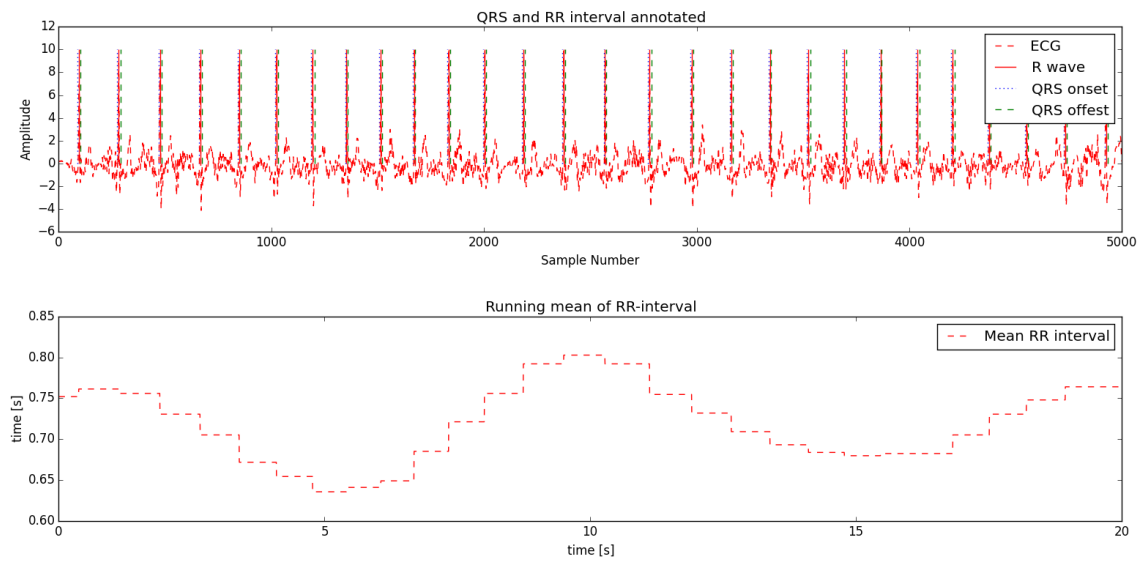


Figure 5-13 R peak approximation

### 5.3.2 RR interval

Since we know the approximate R wave peak location, we can now plot RR-intervals. Figure 5-14 presents the running average of the three consecutive RR-intervals. It can be seen that the RR-interval length varies.



**Figure 5-14 Mean RR interval plot**



## 6 Support Vector Machine for Abnormal Beat Detection

This chapter details the method used for abnormal cardiac beat detection. A one-class Support Vector Machine (SVM) trained on QRS complex samples was used as a classifier since negative examples were not available. The Python code for one-class SVM has been reproduced in Appendix E.

### 6.1 Support Vector Machines

The detection of abnormal cardiac beats is a classification problem. That is, by analyzing each cardiac beat in an ECG record we have to determine whether the beat is normal or abnormal. Since ECG morphologies vary across individuals, therefore to classify a particular individual's cardiac beats as abnormal we need a Machine Learning algorithm that can be trained using that particular individual's ECG. A classifier trained using a large number of "normal" beats from different individuals might not work for another individual. A support vector machine is a classifier which given labeled training data, produces an optimal function which can then be used to categorize new examples. We use a one-class SVM for abnormal cardiac beat detection.

Traditionally SVM is used for binary or multiclass classification. That is, given a dataset we try to determine the class of each element in the dataset by using previous knowledge about the elements known to belong to a particular class. Suppose we have a dataset with points belonging to two different classes, hollow and filled. Figure 6-1 illustrates the dataset.

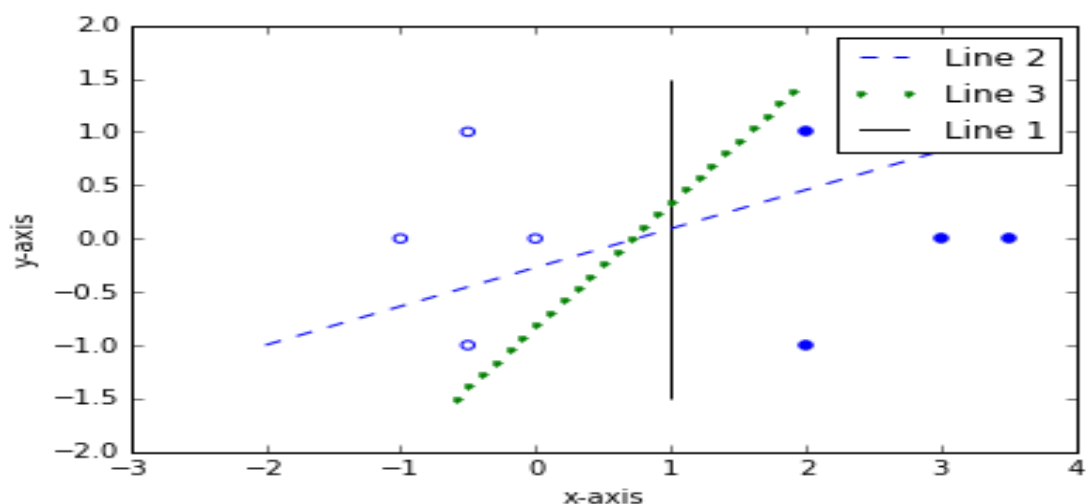
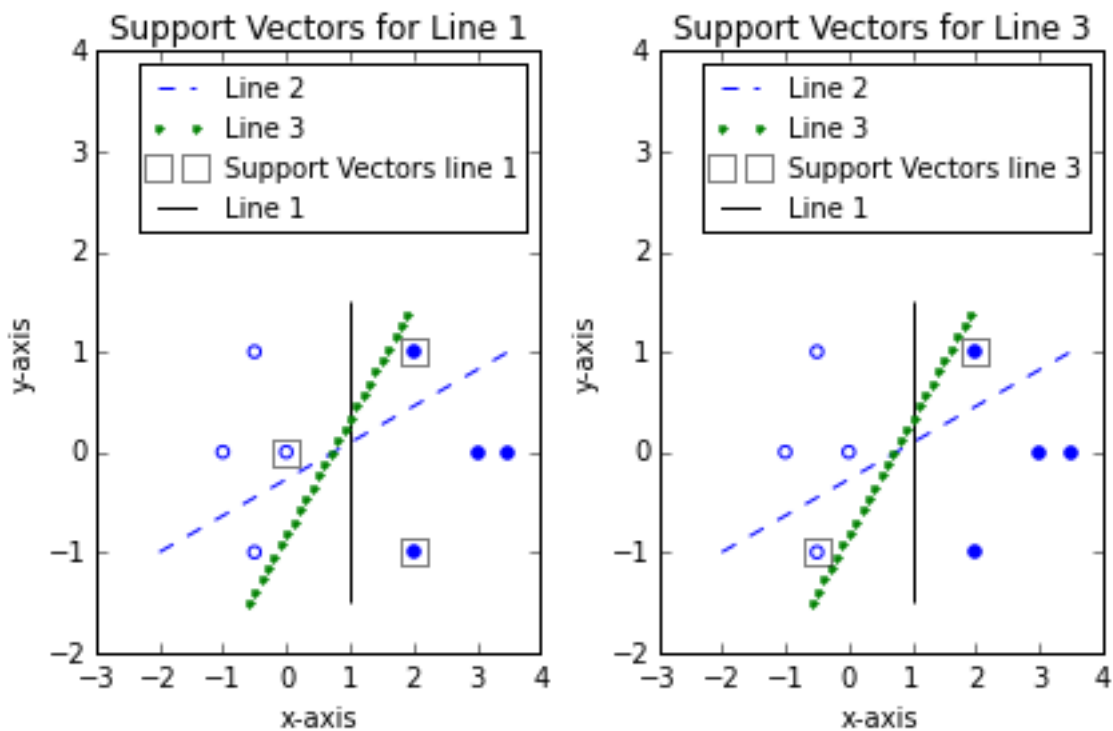


Figure 6-1 Data set with two types of points: hollow and filled.

We can separate the two classes by drawing a line since the data is linearly separable. In Figure 6-1 line 1 and line 3 separate the data while line 2 fails to do so. We can use line 1 and line 3 as classifiers. The optimal classifier however would maximize the perpendicular distance from data points belonging to the two classes since it would reduce the chance of error if a new data point were now to be introduced and classified. The points that lie closest to the separating line in this example are called support vectors. Figure 6-2 marks the support vectors for line 1 and line 3.



**Figure 6-2 Support Vectors**

Support Vector Machines are linear classifiers that produce the optimal separating boundary, line 1 in this case, given a set of labeled training data. Once the separating boundary has been learned, new data points (testing data) can then be classified.

Formally for a two-class support vector machine, consider the data set  $\Omega = \{(x_1, y_1), \dots, (x_n, y_n)\}$  where  $x_i \in R^d$  and  $y_i \in \{-1, 1\}$  and  $y_i$  indicates the class of input vector  $x_i$  [20]. The SVM uses a linear discriminant function to differentiate

between input vectors 'x' belonging to different classes. This linear discriminant function is given in Eq. 6.1.

$$f(x) = \text{sgn}(w^T x + b) \quad (6.1)$$

An SVM training algorithm finds 'w' and 'b' in such a way so as to maximize the margin, as in Figure 6-2, while classifying all the marked training points correctly. That is we need to maximize the margin 'ρ', as in Eq. 6.2, while fulfilling the conditions in Eqs. 6.3 and 6.4 [21].

$$\max \rho = \frac{2}{\|w\|} \quad (6.2)$$

$$w^T x_i + b \leq -1 \quad \forall i \text{ s.t. } y_i = -1 \quad (6.3)$$

$$w^T x_i + b \geq 1 \quad \forall i \text{ s.t. } y_i = 1 \quad (6.4)$$

In order to classify data points which cannot be separated by a linear classifier in their original space  $I$ , the data points are projected to a feature space  $F$  through a non-linear function  $\Phi$  where they can be separated by a hyperplane. The hyperplane projected back to original space  $I$  has the form of a non-linear curve. To avoid over fitting in the presence of noisy data and to provide a solution to the non-linear problem, we use a slack variable  $\xi_i \geq 0$  to allow some data points to lie inside the margin 'ρ'. This is known as soft margin SVM. In general we do not project the input vector to the feature space and use a 'kernel function' which has the same effect [21]. This is known as the 'kernel trick'. Eqs. 6.2 – 6.4 change as in Eqs. 6.5 - 6.6 due to introduction of the slack variable.

$$\min \frac{1}{2} w^T w + C \sum_{i=1}^N \xi_i \quad (6.5)$$

such that

$$y_i(w^T x_i + b) \geq 1 - \xi_i \quad (6.6)$$

The parameter C determines the penalty due to margin violation.

## 6.2 One-class SVM

The previous section was geared towards a general treatment of SVM where we had to differentiate between two or more classes. However, since we only have normal ECG recordings, we need to use one-class SVM. One-class classifiers use training examples from only one class to generate a conception of the data which can then be used to determine whether a new sample point belongs to that class or not.

Formally given training examples  $(z_i, i = 1 \dots N)$ , one-class SVM generates a decision function  $f(z) = w^T \Phi(z) + b$  such that for data in the target class,  $f(z) \geq 0$  while  $f(z) < 0$  for outliers. 'w' is chosen such that the hyperplane  $f(z)$  lies at a maximum perpendicular distance from the origin [22].

Analogous to the parameter C in traditional SVM, one-class SVM uses a parameter 'v' which sets an upper bound on the fraction of outliers in training set and a lower bound on the number of training examples used as support vector.

The approach discussed below uses randomly selected beats from an ECG record to train a one-class SVM algorithm. This particular method has been shown to reach Sensitivity (Se)/Specificity (Sp) of 87.6%/95.8% [23].

## 6.3 Implementation

This section discusses the implementation of one-class SVM used for abnormal beat detection.

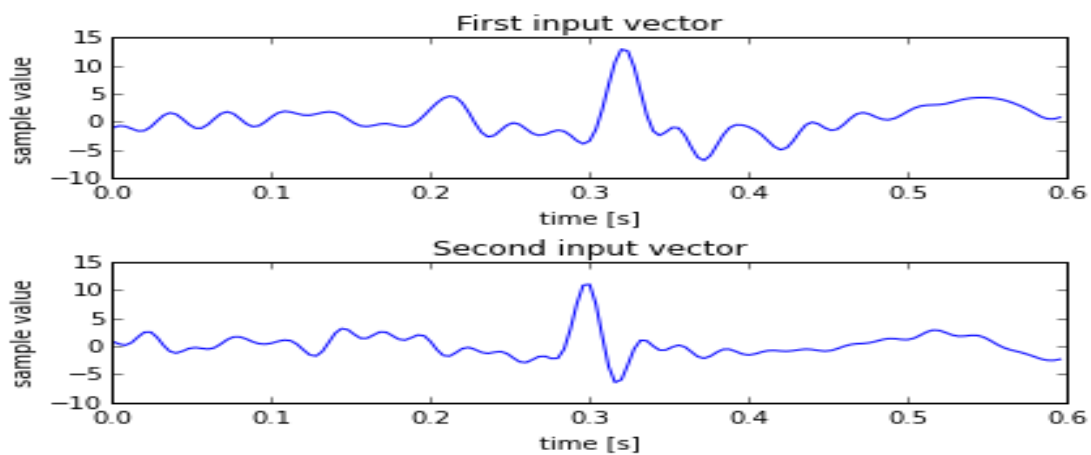


**Figure 6-3 Feature extraction**

### 6.3.1 Feature Extraction

In order to apply one-class SVM we need to extract features from the ECG. We assume that all the beats in the sample are normal. A 0.6 second interval of samples, centered on the R wave, was extracted from randomly selected R waves in the ECG recording. One third of all such samples were used for training while the rest were used for testing. Figure 6-3 presents a sample of the ECG records used for training.

### 6.3.2 Training and Testing

One-class SVM was implemented using scikit-learn, a Python machine learning library. The aforementioned randomly selected ECG records were used as training data while the rest of the samples in the recording were used for testing. The one-class SVM algorithm returns +1 for input vectors classified as belonging to the target class while it returns -1 for outliers. Figure 6-4 presents the results obtained for one ECG recording with a polynomial kernel. Generally with a soft-margin SVM, misclassifications are unavoidable.

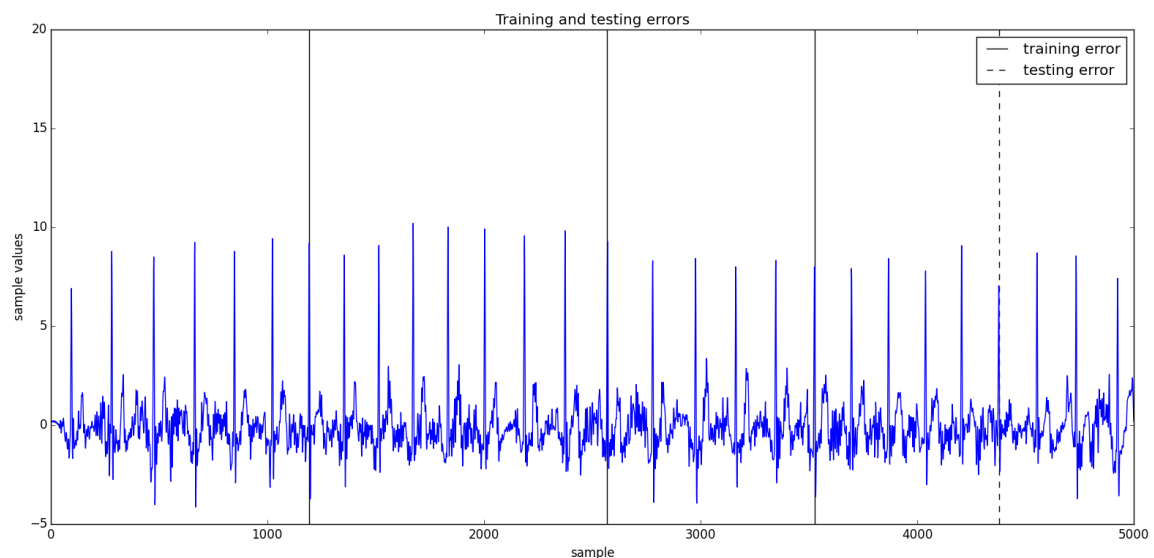


Figure 6-4 Training and testing errors

### 6.3.3 Evaluation

For proper evaluation of one-class SVM, we would need a set of known outliers to test our particular implementation of one-class SVM. Since the ECG data isn't annotated that sort of evaluation isn't possible. In the ideal scenario, we would have an ECG record with abnormal and normal beats annotated by a cardiac expert. In that

case we can calculate sensitivity and specificity to provide a metric for the accuracy of the algorithm.

## 7 Conclusions and Future Work

This work was aimed at the design of an ECG acquisition and analysis system. The main focus of this work has been the implementation of a flexible interface for our acquisition hardware and the detection of QRS complexes for abnormal beat detection. In this chapter we present our conclusions about different techniques implemented in this work along with the issues which can be resolved in another undertaking of a similar nature.

The ECG signal obtained from our acquisition hardware is contaminated with a number of artifacts of which power line interference has proven to be intractable. While analog and digital filtering of the ECG, as discussed above helps, a more robust acquisition circuitry with better common mode rejection ratio and a greater focus on analog filtering can increase the reliability of the acquisition circuitry. Furthermore, the acquisition circuitry currently only provides the option for single lead (lead I) ECG acquisition.

A microcontroller was used to digitize the acquired ECG and to develop a USB interface for our acquisition hardware. We wrote an application to communicate with our acquisition module from a Personal Computer or Laptop. The application allows the user to acquire ECG, view it by generating a plot, saving it to a file and to stream the acquired signal to a remote server. This application has been tested to work on Linux based systems. The development of an application to do the same using an android or other cell phone would greatly enhance the portability of the acquisition module.

Forward backward band pass (0.5 -45 Hz) filtering of the acquired signal was implemented in order to reduce the computational complexity introduced by a high order FIR filter with similar characteristics. The filter successfully removes baseline variations and reduces the noise added through power line interference.

The identification of QRS complexes is a fundamental component of an automated ECG analysis system. The length transform algorithm was used for detection of QRS fiducial points and R wave peak detection. The QRS complex comprises a majority of the curve length of the ECG and the length transform algorithm approximates the

curve length through a simple difference operation of the acquired sample values. The algorithm is reliable but the QRS start and end points can be detected with greater accuracy using other algorithms. The detection of the R wave peak in our system hinges on the correction detection of QRS complex fiducial points since we approximate the R wave peak as the midpoint of the QRS start and end.

The system implements two main diagnostic utilities. First, it allows the user to view the running average of the RR intervals. Secondly, we have implemented a one-class SVM to detect abnormal cardiac beats. Both of these utilities would benefit from a cleaner ECG record. Furthermore, the one-class SVM would function better with a better feature extraction mechanism and a larger ECG record which would provide more data for training. The one-class SVM can be supplemented or replaced by other classification techniques. If annotated ECG training data were available, a binary SVM could be used.

The integrated system can be used as a portable device for long term remote monitoring of cardiac patients. If the android interface were available, the acquisition circuitry along with an android phone could be used to stream an ECG record to a remote server for analysis which can then alert a medical expert if needed. The system can thus be used as portable monitoring system

The analysis algorithms can be coupled with a database of ECG records of different patients for automatic analysis of the ECG. This would reduce the burden on a cardiac expert since the expert could then only review the ECG records flagged by the analysis system.



## Appendix A

### Parameter Setting of ADC

The 10-bit analog to digital converter (ADC) module of PIC18F4550 consists of five registers.

- 1) A/D Result High Register (ADRESH)
- 2) A/D Result Low Register (ADRESL)
- 3) A/D Control Register 0 (ADCON0)
- 4) A/D Control Register 1 (ADCON1)
- 5) A/D Control Register 2 (ADCON2)

The result of an A/D conversion is loaded into ADRESH: ADRESL register pair. The remaining three registers are used to control the operation of analog to digital converter (ADC) module.

The configuration of the three control registers of ADC module for converting analog ECG signal to digital (binary) form are described below with details,

#### A.1 A/D Control Register 0 (ADCON0)

The various bits in the register are shown below in Figure A-1.

U-0	U-0	R/W-0	R/W-0	R/W-0	R/W-0	R/W-0	R/W-0	
—	—	CHS3	CHS2	CHS1	CHS0	GO/DONE	ADON	
bit 7								bit 0

**Figure A-1 ADCON0 Register**

The analog to digital converter (ADC) module of PIC18F4550 has thirteen input channels. Among the available channels we selected channel 0(AN0). Therefore the values for analog channel select bits become,

**CHS3:CHS0**

**0000 = Channel 0 (AN0)**

Initially the module remains disabled so,

$$\mathbf{ADON = 0}$$

The value of  $\overline{GO/DONE}$  doesn't matters if  $ADON=0$ .

$$\mathbf{GO/\overline{DONE} = 0}$$

## A.2 A/D Control Register 1 (ADCON1)

The various bits in the register are shown below in Figure A-2.

U-0	U-0	R/W-0	R/W-0	R/W-0 <sup>(1)</sup>	R/W <sup>(1)</sup>	R/W <sup>(1)</sup>	R/W <sup>(1)</sup>	
—	—	VCFG1	VCFG0	PCFG3	PCFG2	PCFG1	PCFG0	
bit 7								bit 0

**Figure A-2 ADCON1 register**

Since the amplitude of analog ECG signal varies from -1Volts to +1Volts, we have to use external reference voltages for analog to digital converter module. The values for voltage reference configuration bits are,

$$\mathbf{VCFG1 = 1}$$

$$\mathbf{VCFG2 = 1}$$

Since we required only one channel (AN0) to be used for analog input, the values for A/D port configuration bits are,

$$\mathbf{PCFG3:PCFG0 = 0000}$$

## A.3 A/D Control Register 2 (ADCON2)

The various bits in the register are shown below Figure A-3.

R/W-0	U-0	R/W-0	R/W-0	R/W-0	R/W-0	R/W-0	R/W-0	
ADFM	—	ACQT2	ACQT1	ACQT0	ADCS2	ADCS1	ADCS0	
bit 7								bit 0

**Figure A-3 ADCON2 register**

The result of analog to digital conversion was right justified; therefore the value of A/D result format select bit was selected to be,

$$\mathbf{ADFM = 1}$$

The minimum acquisition time for PIC18F4550 was  $0.772\mu\text{s}$ . The microcontroller was operating at 48MHz. Thus the values for A/D acquisition time select bits came out to be,

**ACQT2:ACQT0**

$$111 = 20T_{AD}$$

The A/D conversion clock select bits were selected to be,

**ADCS2:ADCS0**

$$100 = F_{osc}/4$$

## Appendix B

### UNIVERSAL SERIAL BUS (USB)

The universal serial bus (USB) is a high speed serial interface that is used to transmit digital data to a PC. The bus can also power up the devices connected to it. A USB interface is implemented using four wires as discussed below,

**Table B-1 USB wires specification**

Pin	Name	Wire color	Description
1	V <sub>BUS</sub>	Red	+5 Volts
2	D-	White	Data -
3	D+	Green	Data +
4	GND	Black	Ground

PIC18F4550 has a USB peripheral which supports full speed (12Mbps) and low speed (1.5Mbps) communication with any USB host and microcontroller.

#### B.1 Configuration Bits

Configuration bits of a microcontroller allow the user to customize certain aspects of the device to the needs of the application. When the device powers up, the state of these bits determines the modes that the device uses. The settings made for configuration bits during the development of the project are given below,

- External oscillator was selected
- HS,PLL was enabled
- The clock source for USB was set from the output of PLL
- The default values of other configuration bits were used
- Pre-scaler value was set to 5
- Post-scaler value was set to 2

#### B.2 Description of MikroC USB Library Functions

Following MikroC USB library functions were used in the project.

**1 Hid\_Enable (&readbuffer, &writebuffer)**

This function enables the USB communication and requires two arguments: Read buffer address is the location in microcontroller RAM where data sent by host is stored. Write buffer address is the location in microcontroller RAM where data sent by microcontroller is stored. This function must be called before calling any other functions of the USB library.

**2 Hid\_Read ()**

This function receives the data from USB bus and stores in the read buffer. It returns the number of characters received.

**3 Hid\_Write (&writebuffer, length)**

This function sends the data from write buffer to the USB bus. The name of the buffer and the length of the data to be sent must be specified as arguments to the function. The function does not return any data.

**4 Hid\_Disable ()**

This function disables the USB data transfer. It has no arguments and returns no data.

**5 Usb\_Interrupt\_Proc ()**

This function is used for servicing various USB bus events. The function requires no parameters. It must be ensured before using this function that USB interrupts are enabled.

## Appendix C

### Code for USB interface implementation

```

/*----- Description:-----
    The code accomplishes the following tasks,
    1. Converts analog ECG signal to a set of 10-bit digital values.
    2. Transmit the digital ECG signal to a PC using USB.
    * Test configuration:
        MCU(Microcontroller):          PIC18F4550
                                       http://ww1.microchip.com/downloads/en/DeviceDoc/39632D.pdf

        Oscillator:      HS 20.000 MHz (USB osc. is raised with PLL to 48.000MHz)
-----*/

//Buffers should be in USB RAM , please consult datasheet for details
unsigned char readbuff [64] absolute 0x500;
unsigned char writebuff [64] absolute 0x540;

//Variables are used to measure the USB data transfer time and minimize the //variation in
//sampling time
int value;
int new_value;

//Variable used to count the number of conversions
int i;

//-----USB Interrupt Service Routine-----
void interrupt(){
USB_Interrupt_Proc();
}
//-----End of Interrupt Service Routine-----
--

//-----Start of Main Function-----
----
void main()
{
    INTCON = 0x80;           //Enable Interrupts
    ADCON0 = 0x00;         //Initially disabling the analog to digital converter
                          // and selecting channel AN0
    ADCON1 = 0x00;         //Configuring all the ports as analog and setting
                          //internal voltage ref.
    ADCON2 = 0xBC;         //Making the required settings as described in the section
                          //for ADCON2

    T0CON=0x08;           //Required Settings for Timer Zero

```

```

TMR0IE_bit=0;          // Timer Zero Interrupt Disabled

TMR0L=0x00;           //Load Timer Zero with 0
TMR0H=0x00;
i = 0;

label: HID_Enable(&readbuff , &writebuff); //Enable HID Communicatio
while (!HID_Read());           //Wait Unless a read operation is successful
ADCON0 = 0x01;                // Enable ADC
TMR0ON_bit =1 ;              //Start Timer Zero

while (!HID_Read())           //Continue Loop unless a read operation is
                               //successful
{
    GO_DONE_bit = 1;          //Start ADC conversion

    while (GO_DONE_bit == 1); //Wait unless the conversion is complete
    writebuff [i] = ADRESL;    //Write the results of conversion to USB RAM
    writebuff [i+1] = ADRESH;
    i=i+2;

    if (i==64)                //Check that 32 conversions are complete or not
    {

        TMR0L=0x00;          //Load Timer0 with Zero
        TMR0H=0x00;

        while (!HID_Write(&writebuff , 64)); //Send the results of Conversion to PC
        value = TMR0H<<8+TMR0L;              //Read the time for USB
                                                //transfer

        new_value = 65536-24000-value;       //new_time = 2.2ms - time
        TMR0L = new_value;                   //Load Timer0 with new time

        TMR0H = new_value>>8;
        TMR0IF_bit = 0;                     //Set Interrupt Flag to Zero
        while(!TMR0IF_bit);                 //Wait until timer0 interrupt occurs
        i = 0;                               //Set i=0
        continue;                           //Start new conversion by going to the
                                                //top of loop
    }
    delay_us(2200);                        //Sampling Time
}
goto label;
}
//-----End of Main Function-----

```

## Appendix D

### Python code for USB compatible Device

```

'''
The code is written for Python3 and operates correctly when run from the terminal shell on
Linux Ubuntu version 14.04.
'''
# : For one line comments
#''':For multiple line comments
# importing the required modules

import multiprocessing
import usb.core
import usb.util
import matplotlib.pyplot as plt
import socket
import tty,select,sys,termios
import binascii
import struct
import sys
import random

'''
Connect_USB method connects the microcontroller to the PC. The Vendor and Product for the
microcontroller are 0x0001 and 0x1234
respectively. The method searches for the device and then detaches the kernel driver, which
was connected to the device upon connection. The configuration for the device is then set and
addresses for the ENDPOINT IN and ENDPOINT OUT are obtained.
'''

def Connect_USB():
    global dev,reattach,endpoint #Make the variables global

    dev = usb.core.find(idVendor = 0x0001,idProduct = 0x1234)
    #Find the device with the given Vendor and Product ID
    reattach = False

    if dev.is_kernel_driver_active(0):
        #Checks whether the kernel driver is active or not. If kernel driver
        reattach = True
        #is active then detach the kernel driver.
        dev.detach_kernel_driver(0)

    dev.set_configuration()
    #Set the configuration for the device.
    cfg = dev.get_active_configuration()
    intf = cfg[(0,0)]

```



```

endpoint = (dev[0][0][0])

ep = usb.util.find_descriptor(
    intf, custom_match = \
        lambda e:\
            usb.util.endpoint_direction(e.bEndpointAddress)== usb.util.ENDPOINT_IN)

#Addresses for ENDPOINT IN and ENDPOINT OUT

'''
The method Acquire_Data has a queue(Que) as an argument. This method gets the data from the
usb and puts it in the queue after converting the ten bit ADC results into a corresponding
integer.
'''

def Acquire_Data(Que):
    dev.write(0x01,[1])
#Write '1' to the microcontroller so that process of data sending starts
    temp_64 = [] #Empty list to save data
    while (True):
        data = dev.read(endpoint.bEndpointAddress,endpoint.wMaxPacketSize,5000)
#Read data sent by the microcontroller with a timeout=5ms
        length = len(data) #Finding Length of data
        for i in range(int((length-2)/2)):
            temp = [data[2*i],data[2*i+1]]
            num = int.from_bytes(temp,'little',signed = False)
#Converting data bytes to integer
            temp_64.append(num)
            temp_data = list(temp_64) #Copying List to a new list
            Que.put(temp_data) #Writing data to the queue.
            del temp_64[0:] #Deleting items from the list

'''
The method Save_File has also queue as an argument. The data in queue is read and written to
the file.
'''

def Save_File(Que):
    step = 5/1024 #Step used to convert data integers into voltages
    file = open('ecg.txt','w') #Open a file 'ecg.txt' in write mode

    while (True):
        read = list(Que.get()) #Read data from the queue and convert it into list.

        for i in range(len(read)):
            file.write(str(read[i]*step)+'\n')
#Writing to file after making strings of the voltages and appending a new line #characters
'''
The method Stream has also a queue as an argument(Que). A socket is created and connected to
the server ip 192.168.233.107. the communication will happen through the port '10000'. A
structure object packer is created. The argument shows that this structure will operate on a

```

*data that is List with 32 items and items are integers. Packer object is used to pack(convert to binary) the data in values which was read from queue. The binary data is then converted to hex format and sent to the server.*

```
'''
def Stream(Que):
    sock = socket.socket(socket.AF_INET, socket.SOCK_STREAM)
#Create a TCP/IP socket
    server_address = ('192.168.233.107', 10000)
    sock.connect(server_address)          #Connect to socket
    values = Que.get()                    #Read values from the Queue
    packer = struct.Struct('I '*32)      #Creating Packer object
    packed_data = packer.pack(*values)    #Converting Values to binary
    try:

        print ('sending "%s"' % binascii.hexlify(packed_data), values)
#Converting binary data to hex format
        sock.sendall(packed_data)        #Send data through socket

    finally:
        print ('closing socket')
        sock.close()                    #Closing socket

'''
```

*The method Real\_Time\_Plot has also a queue as an argument. The function creates a figure and plots a line corresponding to  $y = 0$  for 1000 points. Limits for the y-axis of the plot are then set to the range '-10' to '10'. The data is then read from the queue and put in y. The data is then updated and plotted*

```
'''
def Real_Time_Plot(Que):
    fig = plt.figure()                  #Create an empty figure
    ax = fig.add_subplot(111)          #Add a subplot to the figure
    y = [0]*1000
    li, = ax.plot(y)                   #Create a plot object later used to plot updated data
    plt.grid(True)                     #Turn grid on
    fig.canvas.draw()

plt.show(block = False)               #Show Plot
plt.ylim((-10,10))                   #Set y-limits
while (True):
    read = qu.get()                   #Read data from queue
    del y[0:len(read)]
    y = y+a
    li.set_ydata(y)                   #Plot updated data
    fig.canvas.draw()
    del read[0:]
'''
```

```

'''
The function isData monitors the terminal for input. If there is an input on the terminal the
function returns 1 otherwise 0.
'''
def isData():
    return select.select([sys.stdin], [], [], 0) == ([sys.stdin], [], [])

'''
The method main gets the setting of the terminal before performing any other task. The method
Connect_USB is called afterwards and if the connection is established 'USB_Connected' is
printed. A multiprocessing queue is then formed which is used to share data between two
processes. Two processes are then created and started which run in parallel. The first process
calls the function Acquire_Data while the second process can call any one of the functions
'Save_File', 'Real_Time_Plot' or 'Stream'. The main then monitors the terminal for input. If
'Esc' key is pressed the main terminates the child processes and also stops the
microcontroller by writing '1' to the microcontroller. In the end, the device is reattached to
the kernel driver.
'''

if __name__ == "__main__":
    old_settings = termios.tcgetattr(sys.stdin) #Get the settings of terminal
    Connect_USB() #Calls the Connect_USB method
    print ('USB_Connected')
    que = multiprocessing.Queue()
#Creates a Queue to share data between processes

    p1 = multiprocessing.Process(target = Acquire_Data, args = (que,))
#Define processes. Target specifies the function to be run as a separate process

    p2 = multiprocessing.Process(target = Stream, args = (que,))
    p1.start() #Start both processes
    p2.start()
    try:
        tty.setcbreak(sys.stdin.fileno())
#Monitors the terminal for input. If 'Esc' key is pressed the finally block executes
        while (True):
            if isData():
                c = sys.stdin.read(1)
                if (c == '\x1b'):
                    break

    finally:
        termios.tcsetattr(sys.stdin, termios.TCSADRAIN, old_settings)
#Reassign the old settings to terminal
    p1.terminate() #Close process 1 and 2
    p1.join()
    p2.terminate()
    p2.join()

```

```

usb.util.dispose_resources(dev)
dev.attach_kernel_driver(0)           #Reattach Kernel driver
print ('USB_Disconnected')

```

```

#-----Server code for Host-----

import binascii
import socket
import struct
import sys

# Create a TCP/IP socket
sock = socket.socket(socket.AF_INET, socket.SOCK_STREAM)
server_address = ('192.168.233.107', 10000)
sock.bind(server_address)
sock.listen(1)           #Server listens to a single client

unpacker = struct.Struct('I '*32) #A structure used to unpack the data sent by client

while True:
    print ('\nwaiting for a connection')
    connection, client_address = sock.accept()
    try:
        data = connection.recv(unpacker.size)
        print ('received "%s"' % binascii.hexlify(data)) #Convert binary to hex format

        unpacked_data = unpacker.unpack(data)
        print ('unpacked:', unpacked_data)

    finally:
        connection.close()           #Close Connection

```

# Appendix E

## Python Code for ECG Analysis

```

from scipy import signal, ndimage
from numpy import array,diff, append,int8,where,mean, int32, floor, std
import numpy as np
from numpy import ones as np_ones
from matplotlib import pyplot as plt
from random import randint
from sklearn import svm
#-----Read ECG function-----
def read_ecg():
    file_name = input("Please enter path and name of file ")          #Recorded ECG file
    if file_name == '':
        file = open ('D:\\University\\7th Semester\\FYP\\python\\hasan1_ecg.txt','r')
    else:
        file = open (file_name, 'r')
    ecg_sig = []                                                    #For reading data from file
    for i in file:
        ecg_sig.append(int( file.readline() ) )
    file.close()
    return ecg_sig
#----- Block Processing function (mean) -----
def funm(data,length):
    '''funm(data,length) takes mean of each window of length "length" in data.
    Data should be a list
    inputs:
        data - a list containing data points
        length - window length for mean calculation
    output:
        z - a list of length "len(data)" with elements replaced by mean of elements
            falling in each window of length "length"

    example:

    >>> z = funm([1,2,3,4,5] , 2)
    >>> print(z)
    [1.5, 1.5, 3.5, 3.5, 5.0]
    ...

    z = []
    number = floor(len(data) / length)
    zeros = int32((len(data) - number*length ))

    for i in range(int32(number)):
        block = data [i*length:(i+1)*length]

```

```

        ones = length*[mean(block)]
        z.extend(ones)
    lst_mean = mean(data[-zeros:])
    ones = zeros*[lst_mean]
    z.extend(ones)
    return z
#----- Block Processing function (standard deviation) -----
def funs(data,length):

    '''funs(data,length) takes mean of each window of length "length" in data.
    Data should be a list
    inputs:
        data - a list containing data points
        length - window length for mean calculation
    output:
        z - a list of length "len(data)" with elements replaced by standard deviation of
elements
        falling in each window of length "length"

    example:

    >>> z = funs([1,2,3,4,5] , 2)
    >>> print(z)
    [1.5, 1.5, 3.5, 3.5, 5.0]
    ...

    z = []
    number = floor(len(data) / length)
    zeros = int32((len(data) - number*length ))

    for i in range(int32(number)):
        block = data [i*length:(i+1)*length]
        ones = length*[std(block)]
        z.extend(ones)
    lst_std = std(data[-zeros:])
    ones = zeros*[lst_std]
    z.extend(ones)
    return z
#-----QRS detection function -----
'''
def QRS_LT (samp, ecg_sig,noise_fac = 0.5):
    ''' QRS_LT(samp,ecg_sig,noise_fac) implements the length transform method
    for QRS detection based on a simple derivative approach.

    inputs:
        samp: sampling frequency
        ecg_sig: a list (not np.array) containing ecg data points
'''

```

```

noise_fac: a factor which can be used to suppress the effects of noise
          on QRS detection. For high noise, choose a noise factor closer to 1.
          The default value is zero.
outputs:
  index_on: list containing sample numbers indicating start of a QRS
  index_off: list containing sample numbers indicating end of a QRS

Note that the two lists are populated such that we first count a QRS starting
point and then the ending point. This means that if ecg_sig contains a QRS
ending point without a starting point, it will be neglected.
...
MF = 2.0
qrs_size = 0.12*samp
min_qrs_size = 0.04*samp
nyq = samp/2
#----- Bandpass filtering -----
coeff = signal.firwin2 (101, [0, 8/nyq, 10/nyq, 25/nyq, 27/nyq, 35/nyq, nyq/nyq],
[0,0.7,1,1,0.7,0,0], window = 'blackman')
initial = 100
delay = (initial // 2)                                     #Remove delay introduced by
FIR filter
ecg_sig.extend(delay*[0])                                  #Append zeros equal to delay at the end
ecg_sig = signal.lfilter (coeff, 1, ecg_sig)              #Filter
ecg_sig = ecg_sig[delay:]                                  #Remove delay so that filtered and original
                                                         #data line up

#----- Differentiation and squaring -----
ecg_sig = diff (ecg_sig)
# h = array([-2, -1, 1, 2])/8

ecg_sig = append(ecg_sig,[0])
ecg_sig = [i**2 for i in ecg_sig]

#----- Thresholding -----
T_win = 4*samp
threshold = funm(ecg_sig,T_win)
#Call block processing function(mean) with window length T_win
noise_fac = noise_fac*max(threshold)
threshold = noise_fac + MF*array(threshold)
decision = (ecg_sig > threshold )
decision.dtype = int8

#-----Morphological closing and opening -----
struct_close = np_ones(qrs_size)
#structure for morphological closing
decision = ndimage.morphology.binary_closing(decision,struct_close)
decision.dtype = int8
#function returns bool

```

```

struct_open = np_ones(min_qrs_size)          #structure for morphological opening
decision = ndimage.morphology.binary_opening(decision,struct_open)
decision.dtype = int8
#function returns bool
    decision1 = append(diff(decision), [0])
#after difference: 1 denotes start of QRS, -1 end of QRS (plot it)

#-----Find indices -----
    index_on = where(decision1 == 1)          #returns tuple
    index_on = index_on [0]
#first element of tuple contains the array of our interest
    index_off = where(decision1 == -1)
    index_off = index_off [0]

    if (len(index_on) > 0 and len(index_off) > 0):          #Non-empty
        if (index_off[1] < index_on[1]):
            index_off [1] = []
#ECG starting index < ECG closing index
        if (len(index_off) == 0 or (index_on[-1] > index_off[-1])):
            index_on [-1] =[]
#Again only sets of QRS onset and offest are being included
    else:
        index_on = []
        index_off = []

    return index_on, index_off

#-----Band pass filter-----
def bandpass_filter(samp, ecg_sig):
    ...
    bandpass filters the signal using chebyshev filter of order using forward
    backward filtering

    input:

    samp: sampling frequency in Hz
    ecg_sig : Signal to be filtered

    output:

    response: forward backward filtered ecg_sig
        b = np.array([ 0.06876288, -0.42392463,  1.19560393, -2.12170399,  2.69859612,
-2.50278218,  1.48077995,  0.          , -1.48077995,  2.50278218,
-2.69859612,  2.12170399, -1.19560393,  0.42392463, -0.06876288])
    a = np.array ([ 1.00000000e+00, -8.49604161e+00,  3.35577780e+01,
-8.22283201e+01,  1.40439389e+02, -1.77470173e+02,
 1.71326048e+02, -1.28356988e+02,  7.49712127e+01,
-3.39410935e+01,  1.16939037e+01, -2.95566529e+00,
 5.02936968e-01, -4.13786796e-02, -1.60836561e-03])

```



```

...

from scipy import signal

nyq = samp/2
b,a = signal.iirdesign ([2/nyq, 40/nyq], [0.5/nyq, 45/nyq],1,30)
response = signal.filtfilt(b,a, ecg_sig)
return response

#----- RR_interval -----

def rr_interval(index_on, index_off):

    ...

    rr_interval(index_on, index_off) simply returns the average of the corresponding
    elements of index_on and index_off

    Inputs:
    index_on: A np.ndarray containing sample numbers corresponding to the start of a QRS
    complex
    index_off: A np.ndarray containing sample numbers corresponding to the end of a QRS complex

    Output:
    rr_interval: A np.ndarray containing the average of corresponding samples in the input
    arrays

    Please note the function only works if all the elements in index_on are smaller than the
    corresponding
    elements in index_off and the length of the two arrays is equal.

    ...

    rr_int = np.array([])
    if ( (index_on < index_off).all() and len(index_on) == len (index_off)):

        for i in range (len(index_on)):
            rr_int = np.append( rr_int , (index_on[i] + index_off[i])/2)

    return rr_int

#----- Block Processing of RR-Intervals-----

def rr_block (rr_int, no_of_samples):

    ...

    rr_block (rr_int, no_of_samples) block processes the elements in rr_int (takes block mean
    of 3 rr_intervals)
    and returns an np.array equal to the length of rr_int.

    inputs:

```

```

rr_int: Input list/np.array containing the sample point of an R in an ECG signal.
no_of_samples: Total number of samples of the ECG signal for which the RR_intervals
are to be calculated.

output:
An np.array 'c' which contains the average of three consecutive RR intervals
generated from rr_int.
...

interval_length = diff(rr_int)
#Calculate rr_interval length
c = np.array([])
c = np.append(c , interval_length [0] *(np.ones(rr_int [0])))
#Array which holds average of each block of 3 RR - intervals
number = len(interval_length) // 3
zeros = len(interval_length) - number*3

for i in range (0, number*3, 3):
    mean_value = (interval_length [i] + interval_length [i+1] + interval_length [i+2])/3
#Take mean
    time_average_gen = mean_value*np.ones((rr_int[i+3] - rr_int[i]))
    c = np.append (c, time_average_gen)

mean_value = mean(interval_length[-zeros:])
c = np.append(c, mean_value*(np.ones((no_of_samples - rr_int[number*3])))
return c

#-----Running mean-----

def moving_average(rr_int, total_samples, length = 3):
    ...

    mvoing_average() calculates the moving average of samples
    in rr_int and returns an array c containing the running
    average of the rr_intervals which can be directly plotted
    ...

    interval_length = diff(rr_int) #Calculate rr_interval length
    weights = np.repeat(1.0, length)/length
    mov_average = np.convolve(interval_length,weights,'valid')
#Moving average of RR intervals
    boundary = np.array([mean(interval_length[-2:]), interval_length[-1]])

#Handle conditions at the boundary of the interval_length array
    mov_average = np.append(mov_average,boundary)
    c = np.array([])
    c = np.append(c , interval_length [0] *(np.ones(rr_int [0])))
    for i in range(0,len(mov_average)):
        c = np.append(c,mov_average[i]*np.ones(rr_int[i+1]-rr_int[i]))
    c = np.append(c, mov_average[-1] * np.ones(total_samples - rr_int[-1]))
    return c

```

```

#-----Extract samples for ONE CLASS SVM-----
def extract_samples(ecg_sig, samp, rr_int):
    '''extract_samples(ecg_sig,samp,rr_int) extracts 0.6 seconds intervals around
    each R wave and returns an array (numpy) of arrays which contains intervals
    corresponding to each R wave.

    output:
    qrs: extracted qrs complex samples
    sample_numbers: Start and end point of extracted QRS complexes
    ...

    intervals = []
    qrs_sample_numbers = []
    for i in range(0, len(rr_int)):
        if i == 0:
            if (rr_int [i] - int(samp*0.3)) >= 0:
                intervals.append(ecg_sig[int(rr_int [i]) - int(samp*0.3) : int(rr_int [i]) +
int(samp*0.3)])
                qrs_sample_numbers.append([int(rr_int [i]) - int(samp*0.3) , int(rr_int [i]) +
int(samp*0.3)])
            elif i == len(rr_int)-1:
                if( rr_int [i] + 0.3*samp) < len(ecg_sig):
                    intervals.append( ecg_sig [int(rr_int[i]) - int(samp*0.3): int(rr_int[i]) +
int(samp*0.3)])
                    qrs_sample_numbers.append([int(rr_int [i]) - int(samp*0.3) , int(rr_int [i]) +
int(samp*0.3)])

            else:
                intervals.append( ecg_sig [int(rr_int[i]) - int(samp*0.3): int(rr_int[i]) +
int(samp*0.3)])
                qrs_sample_numbers.append([int(rr_int [i]) - int(samp*0.3) , int(rr_int [i]) +
int(samp*0.3)])
    return intervals, qrs_sample_numbers

#-----ONE CLASS SVM-----
def outlier_detection(qrs, rr_int):
    ...

    outlier_detection (qrs, rr_int) trains a one-class SVM with 1/3
    of the samples in qrs for training and the rest for testing.

    index_test contains indexes of "qrs" used for training
    ...

    length = int(len(qrs)/3) + 2
    index_train = []
    index_test = []
    for i in range (length):
        random_number = randint(0,len(qrs))
        if (random_number not in index_train):
            index_train.append(randint(0, len(qrs)-1))

```

```

index_train.sort()

X_train = []
X_test = []
for i in range(len(qrs)):
    if (i in index_train):
        X_train.append(qrs[i])
    else:
        X_test.append(qrs[i])
        index_test.append(i)

classifier = svm.OneClassSVM(nu = 0.01, kernel = 'poly', gamma = 1, degree = 2)
classifier.fit(X_train)
pred_train = classifier.predict(X_train)
pred_test = classifier.predict(X_test)
error_train = where (np.array(pred_train) == -1)           #Find indexes with -1
error_test = where (np.array(pred_test) == -1)           #Find indexes with -1
errors_train = []
errors_test = []
train_error = []

    #Sample number of QRS complexes which used for training and returned errors
test_error = []
#Sample number of QRS complexes which used for testing and returned errors
if (len(error_train[0]) != 0):
    for h in range(error_train[0][-1]+1):                 #returns tuple
        if (h in error_train[0]):
            errors_train.append(index_train[h])
        errors_train.sort()

    for h in errors_train:
        current = rr_int[h]
        train_error.append(current)

if (len(error_test[0]) != 0):
    for z in range(error_test[0][-1]+1):
        if (z in error_test[0]):
            errors_test.append(index_test[z])
        errors_test.sort()

    for b in errors_test:
        current = rr_int[b]
        test_error.append(current)
return train_error, test_error

#-----
samp = 500
ecg_sig = read_ecg()
x = list(ecg_sig)

```

```

ecg_sig = bandpass_filter (samp, list(map(lambda x :x,ecg_sig )) )
ecg_sig = ecg_sig.tolist()
ecg_sig1 = list(ecg_sig)
index_on, index_off = QRS_LT (samp,ecg_sig1)
rr_int = rr_interval (index_on, index_off)
mean_interval = (moving_average (rr_int, len(x)))/samp
time = (np.arange (0, len(ecg_sig))/samp).tolist()

plt.figure()
plt.subplot(211)
plt.vlines (rr_int, 0, 10, color = 'red', linestyle = 'solid', label = 'R wave')
plt.vlines (index_on,0,10, color = 'blue', linestyle = 'dotted', label = 'QRS onset')
plt.vlines (index_off,0,10, color = 'green', linestyle = 'dashed', label = 'QRS offest')
plt.plot(ecg_sig, 'r--', label = 'ECG')
plt.xlabel ('Sample Number')
plt.ylabel ('Amplitude')
plt.title('QRS and RR interval annotated')
plt.legend()
plt.subplot(212)
plt.plot (time, mean_interval, 'r--', label = 'Mean RR interval' )
plt.ylabel('time(s)')
plt.xlabel('time(s)')
plt.title('Running mean of RR-interval')
plt.legend()
plt.tight_layout()
plt.show()

qrs, sample_numbers = extract_samples (ecg_sig, samp, rr_int)
train_error, test_error = outlier_detection(qrs, rr_int)

```

## References

- [1] A. Alwan, "Global status report on noncommunicable diseases," World Health Organization, 2010.
- [2] M. Hussain, N. Khan, M. Uddin and M. M. A. Nozha, "Chest Pain, Coronary Artery Disease and Risk Factors:A Global Snapshot," *Journal of the Dow University of Health Sciences Karachi*, vol. 8, no. 2, pp. 80-86, 29 September 2013.
- [3] T. Diehl, *ECG Interpretation made Incredibly Easy!*, Pennsylvania: Lippincott Williams & Wilkins, 2011.
- [4] R. Yazicioglu, C. V. Hoof and R. Puers, *Biopotential Readout Circuits for Portable Acquisition Systems*, Springer, 2009.
- [5] Enrique, "ECG Front-End Design is Simplified with MicroConverter®," *Analog Dialogue*, vol. 37, no. 4, pp. 10 - 14, 2003.
- [6] A. Sedra and K. Smith, *Microelectronic Circuits*, 6th Edition, Oxford University Press, 2009.
- [7] A. Devices, "AD 620: Low drift, Low power Instrumentation Amplifier," [Online]. Available: <http://www.analog.com/en/specialty-amplifiers/instrumentation-amplifiers/ad620/products/product.html>. [Accessed 1 January 2015].
- [8] T. Instruments, "LF353," [Online]. Available: <http://www.ti.com/product/lf353>. [Accessed 1 January 2015].
- [9] Microchip, "PIC18F4550," [Online]. Available: <http://www.microchip.com/wwwproducts/Devices.aspx?dDocName=en010300>. [Accessed 1 January 2015].

- [10] Compaq, HP, Intel, Lucent, Microsoft, NEC Philips, "Universal Serial Bus," 27 April 2000. [Online]. Available: [sdphca.ucsd.edu/Lab\\_Equip\\_Manuals/usb\\_20.pdf](http://sdphca.ucsd.edu/Lab_Equip_Manuals/usb_20.pdf). [Accessed 1 January 2015].
- [11] A. Bhat, V. Kumar and S. Kumar, "Design of ECG Data Acquisition System," *International Journal of Advanced Research in Computer Science and Software Engineering*, vol. 3, pp. 676-680, April, 2013.
- [12] B. Lathi, *Modern Digital and Analog Communication Systems*, 3rd Edition, New York: Oxford University Press, 1998.
- [13] "Sound Card Bipolar Voltage to Frequency," Interstellar Research, 2007. [Online]. Available: [http://www.daqarta.com/dw\\_kkvv.htm](http://www.daqarta.com/dw_kkvv.htm). [Accessed 1 January 2015].
- [14] "LM231A/LM231/LM331A/LM331 Precision Voltage-to-Frequency Converters," Texas Instruments, March 2013. [Online]. Available: <http://www.ti.com/lit/ds/symlink/lm331.pdf>. [Accessed 1 January 2015].
- [15] A. M. a. M. J. S. Kasar, "Performance of Digital filters for noise removal from ECG signals in Time domain," *International Journal Of Innovative Research In Electrical, Electronics, Instrumentation And Control Engineering*, vol. 2, no. 4, pp. 1352-1355, 2014.
- [16] V. Romero, "ECG baseline wander removal and noise suppression analysis in an embedded platform," Universidad Complutense de Madrid, [Online]. Available: [URL:http://eprints.ucm.es/9886/1/ECG\\_baseline\\_wander\\_removal\\_and\\_noise\\_suppression\\_in\\_an\\_embedded\\_platform.pdf](http://eprints.ucm.es/9886/1/ECG_baseline_wander_removal_and_noise_suppression_in_an_embedded_platform.pdf). [Accessed 1 May 2015].
- [17] J. Smith, "Introduction to Digital Filters with Audio Applications," Center for Computer Research in Music and Acoustics (CCRMA), Stanford University, 2007. [Online]. Available: URL: <http://ccrma.stanford.edu/~jos/filters/>. [Accessed 1 May 2015].
- [18] V. Afonso, "ECG QRS Detection," in *W.J. Tompkins, eds. Biomedical Digital*

*Signal Processing*, New Jersey, Prentice Hall, pp. 236-264.

- [19] G. M. D. J. W. Zong, "A Robust Open-source algorithm to Detect Onset and Duration of QRS Complexes," in *Computers in Cardiology*, 2003.
- [20] R. Vlasveld, "Introduction to One-Class Support Vector machines," 12 July 2013. [Online]. Available: <http://rvlasveld.github.io/blog/2013/07/12/introduction-to-one-class-support-vector-machines/>. [Accessed 1 May 2015].
- [21] E. Alpaydin, *Introduction to Machine Learning*, London, England: The MIT Press, 2010.
- [22] K. C. S. F. e. a. P. Li, "An Abnormal ECG Beat Detection Approach for Long-Term Monitoring of Heart Patients Based on Hybrid Kernel Machine Ensemble," in *Multiple Classifier Systems*, Springer, 2005, pp. 346-355.
- [23] F. A. Afsar, "A new novelty detector for finding abnormal beats in ECG recordings," in *International conference on Integrative Biology summit*, Las Vegas, 2013.